Supplement of Atmos. Chem. Phys., 26, 2893–2919, 2026
https://doi.org/10.5194/acp-26-2893-2026-supplement

Atmospheric Chemistry and Physics
Open Access
EGU

Supplement of

Measurement report: Emission factors and organic aerosol source apportionment of shipping emissions in the coastal city of Toulon, France

Quentin Gunti et al.

Correspondence to: Quentin Gunti (quentin.gunti@univ-amu.fr) and Barbara D'Anna (barbara.danna@univ-amu.fr)

Contents

List of Figures

List of Tables

S1 Additional technical information on instrumentation

This section provides complementary details on the main instruments deployed during the Toulon campaign, their measurement principles, calibration procedures, and data quality assurance. It also includes contextual information about the measurement site, nearby emission sources, and local meteorology.

All instruments were installed inside the *Massalya* mobile laboratory and operated continuously throughout the campaign. A single stainless-steel inlet was used for all aerosol instruments, with a total flow of 10 L·min^{-1}, corresponding to a residence time of $\approx$ 2.3 s. The sampling line was dried below 40 % relative humidity using a Nafion dryer (Perma Pure), ensuring stable transmission efficiency. The HR-ToF-AMS, SMPS, MAAP, and AE33 shared the same inlet to guarantee identical sampling conditions. Weekly zero and span checks were performed on all analyzers, and the instrument clocks were synchronized with a time offset < 1 s.

S1.1 HR-ToF-AMS (Aerodyne Research Inc.)

The High-Resolution Time-of-Flight Aerosol Mass Spectrometer (HR-ToF-AMS) quantified the non-refractory PM_1 species (organics, sulfate, nitrate, ammonium, chloride) in V-mode with a 30 s time resolution (DeCarlo et al., 2006). Particles were focused by a multi-lens aerodynamic system transmitting efficiently between 70–700 nm vacuum aerodynamic diameter (Liu et al., 2007). The vaporizer was operated at 600 °C under a lens pressure of 1.8×10^{-5} Torr, with 70 eV electron-impact ionization and a mean resolving power of $m/\Delta m \approx 4000$. The instrument vacuum was maintained at 2×10^{-6} Torr in the flight chamber.

Ionization efficiency (IE) calibrations were performed before and after the campaign using size-selected ammonium nitrate and ammonium sulfate aerosols following Jayne et al. (2000); DeCarlo et al. (2006). Relative ionization efficiencies (RIEs) applied were 3.91 (NH_4^+), 1.7 (SO_4^{2-}), 1.1 (NO_3^-), 1.3 (Cl^-), and 1.0 (organics) (Canagaratna et al., 2007). High-resolution analysis and peak fitting were conducted with the `SQUIRREL` v1.65B and `PIKA` v1.25B software packages (Aiken et al., 2007, 2008). The Collection Efficiency (CE) was calculated by comparison with co-located SMPS and MAAP data, following the parameterization of Middlebrook et al. (2012). An average CE of 0.63 $\pm$ 0.09 was applied to ambient data, while CE = 1.0 was used during ship-plume events, consistent with Quinn et al. (2006); Bahreini et al. (2009); Voliotis et al. (2021). The total uncertainty in AMS mass concentrations was estimated at $\pm$14 %, consistent with previous intercomparisons (Brendan M. Matthew and Onasch, 2008; Middlebrook et al., 2012).

S1.2 Site maps and campaign overview

Figure S1. Localization of the Massalya platform at the port of Toulon on the Mediterranean French coast (top), localization of the ferry and cruise ship terminals (down), green lines represent major shipping lines. Map background data sources: ESRI, HERE, Garmin, INCREMENT P, © OpenStreetMap contributors, and the GIS user community Powered by ESRI. Administrative boundaries: Communes of the Métropole TPM.

Figure S2. Localization of the main roads around the measurement site. Map background data sources: ESRI, HERE, Garmin, INCREMENT P, © OpenStreetMap contributors, and the GIS user community Powered by ESRI. Administrative boundaries: Communes of the Métropole TPM.

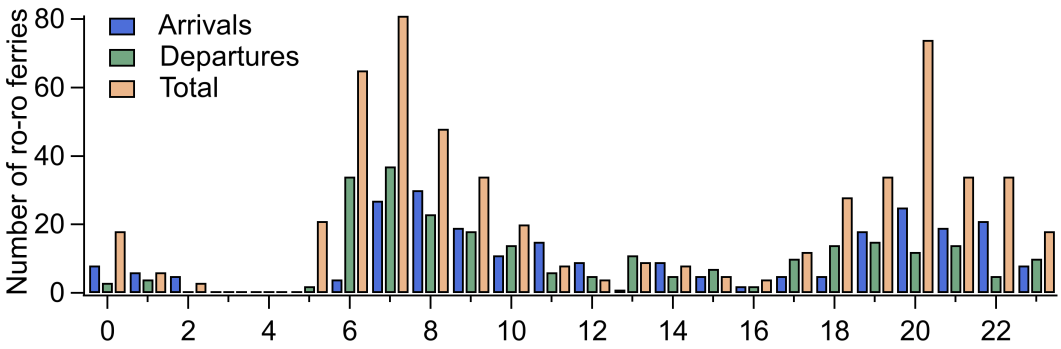

Figure S3. Hourly distribution of arrivals and departures of roro-ferries recorded by the harbor autority.

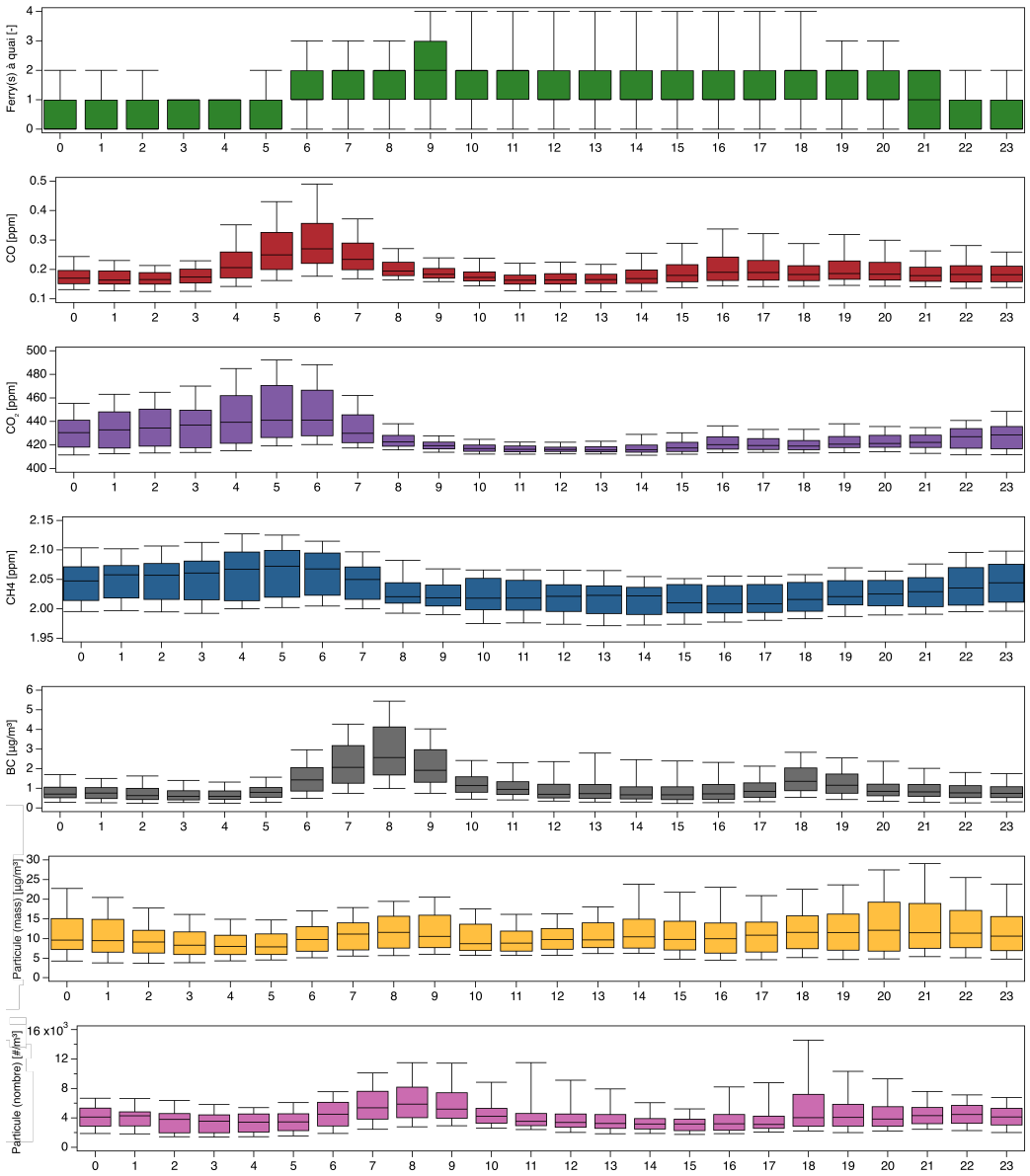

Figure S4. Diurnal distribution of CO, CO_2, CH_4, BC, PM and PN during the campaign.

S1.3 Emission factor calculation methodology

I.3.1) Example of EF calculation

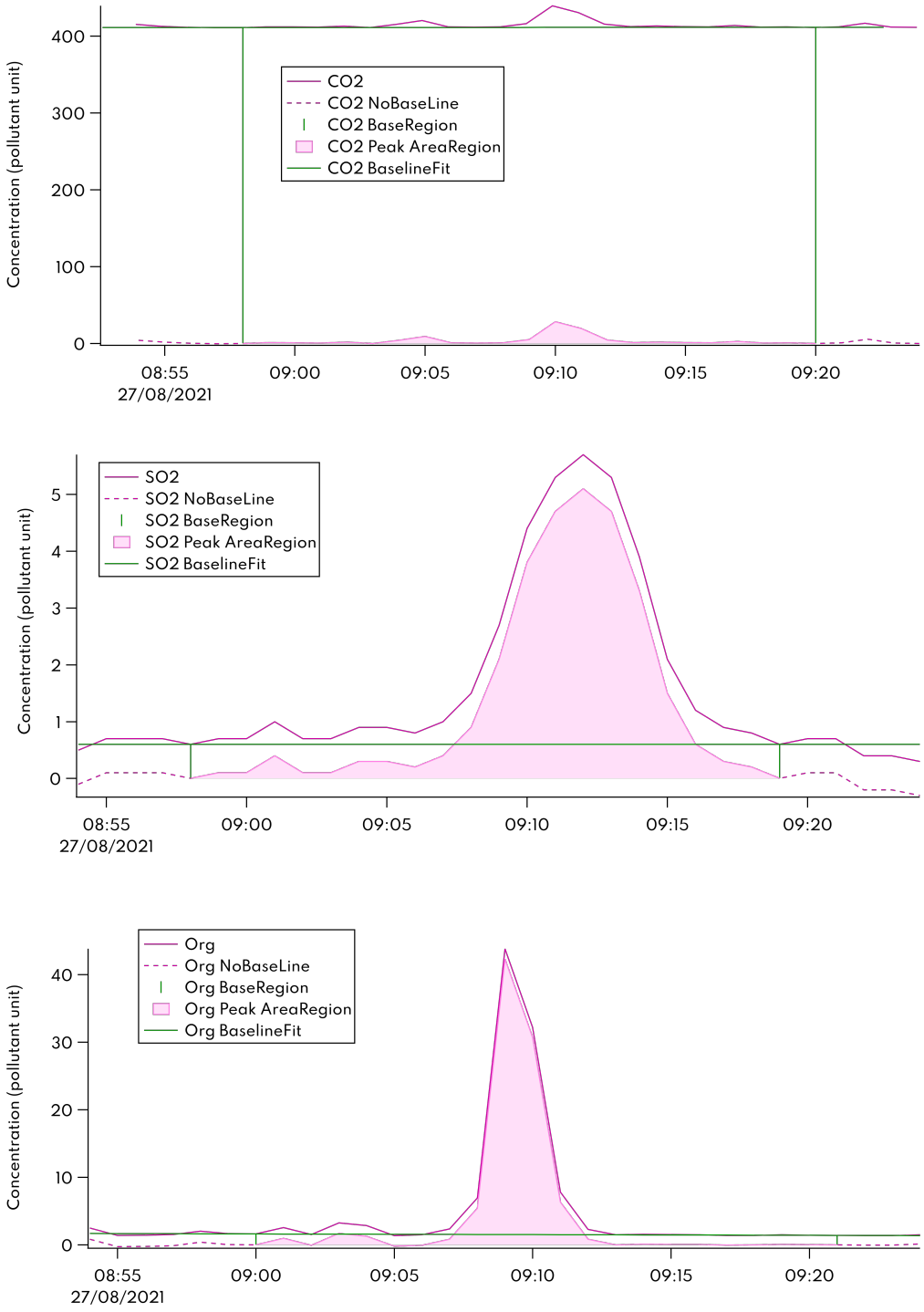

Figure S5. Example of a ship plume event processed with the EF calculation tool developed by Lise Le Berre (Le Berre et al., 2024). Each panel shows the time series of a pollutant (SO_2, CO_2, and organics) during the same plume. The pink area represents the excess concentration integrated to compute the emission factor (EF) after linear background interpolation (green horizontal line). Green vertical lines indicate the start and end of the plume integration window. The tool automatically determines plume boundaries, background fit, and integration areas to derive consistent EFs from transient events using the carbon mass balance method.

Table S1. Type and number of ships mooring in the port area of Toulon.

Type	Number	Proportion
Ferries	285	78.5%
Cruise ships	9	2.5%
Tankers	9	2.5%
Other	25	6.9%
Yachts	19	5.2%
Unspecified	16	4.4%

I.3.2) Summary tables of ship activity and EFs

Table S2. Emission factors of identified ferry plumes. NO_x, NO and CO in g per kg of fuel consumed. SO_2, CH_4, SO_4, Org and PAHs expressed in in mg per kg of fuel consumed and PN in particle per kg of fuel consumed.

Ferries EFs	NO_x	NO	CO	SO_2	CH_4	SO_4	Org	BC	PAHs	PN
Median	18.3	7.1	18.3	318	780	77	1122	261	8	3.08E+15
Mean	25.0	10.0	21.0	508	1006	106	1605	423	11	5.17E+15
Standard-deviation	18.9	8.5	11.9	596	998	108	1430	423	11	4.73E+15
1st quartile	9.8	2.6	13.4	97	273	32	534	156	3	1.44E+15
3rd quartile	35.2	15.9	25.4	611	1248	147	2450	638	15	8.21E+15
Number	34	34	39	41	33	36	41	32	41	40

Table S3. Characteristics of most identified ferries, named A, B, C, D and E (from local port authority).

Ferry	Tier	Main engine	Auxiliary Engine	Fuel Type	Tonnage (GT)	Scrubber
A	II	4×6,600 kW	4×2,045 kW	LSHFO / MGO	40,000	no
B	II	4×12,600 kW	3×2,460 kW	VLSFO / MGO	42,000	no
C	II	4×7,920 kW	3×1,680 kW	VLSFO / MGO	36,000	no
D	I	4×5,750 kW	3×2,045 kW	VLSFO / MDO(1)	24,000	no
E	II	4×11,700 kW	3×1,680 kW	LSHFO / MDO	37,000	no

(1) Switch from MGO to MDO during the campaign.

I.3.3) Comparison with literature EFs

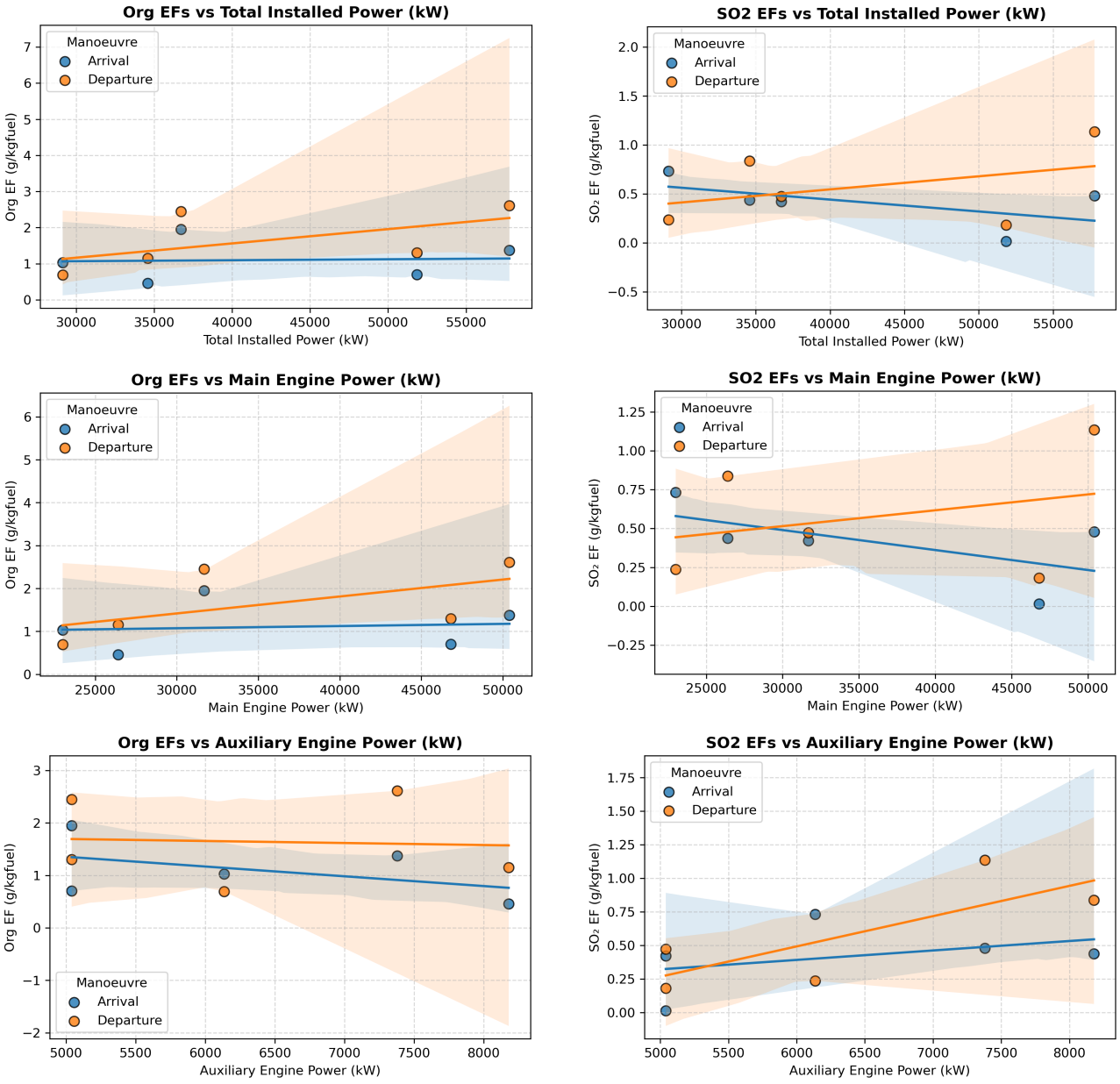

Figure S6. Relationships between emission factors (EFs) of sulfur dioxide (SO_2, right column) and organic aerosol (Org, left column) and ship engine power for the five identified ferries (A–E) during arrivals (blue) and departures (orange). Rows correspond respectively to (top) total installed power, (middle) main engine power, and (bottom) auxiliary engine power. Shaded areas represent 95 % confidence intervals of the linear regressions. A moderate correlation is observed between SO_2 EFs and auxiliary engine power ($R^2 = 0.35$ overall, $R^2 = 0.60$ during departures), while no significant relationship is found for Org EFs ($R^2 < 0.2$). Regression statistics for each configuration are provided in Table S3.

Table S4. Regression parameters between instantaneous emission factors (EFs) and engine power for and organic aerosol (Org) during arrival and departure phases, separated by main and auxiliary power use. Slopes are expressed in g kg_{fuel}^{-1} kW^{-1}, SE denotes the standard error, and R^2 the coefficient of determination.

Pollutant	Power type	Manoeuvre	Slope (g kg_{fuel}^{-1} kW^{-1})	SE	R^2
SO_2	Auxiliary	Arrival	7.03×10^{-5}	9.77×10^{-5}	0.15
	Auxiliary	Departure	2.25×10^{-4}	1.05×10^{-4}	0.60
	Main	Arrival	-1.29×10^{-5}	9.55×10^{-6}	0.38
	Main	Departure	1.02×10^{-5}	1.82×10^{-5}	0.09
Org	Auxiliary	Arrival	-1.86×10^{-4}	2.16×10^{-4}	0.20
	Auxiliary	Departure	-3.85×10^{-5}	3.46×10^{-4}	0.00
	Main	Arrival	5.07×10^{-6}	2.74×10^{-5}	0.01
	Main	Departure	3.95×10^{-5}	3.25×10^{-5}	0.33

Table S5. Summary of literature emission factors (EFs) reported in the literature for comparison with the present study. Unless otherwise specified, values are expressed in g kg_{fuel}^{-1}. For each pollutant, the table lists the reported EF (mean, median, or range), the fuel or engine type, and the corresponding reference.

Pollutant	Reported EF	Fuel / Engine type	Reference
SO_2	26 ± 6	HFO (2.7 % S)	Celik et al. (2020)
	7.7 ± 6.7	HFO / MDO	Diesch et al. (2013)
	2.9 ± 0.2	MDO (0.1 % S)	Sinha et al. (2003)
	0.4 (0.1–0.7)	LSHFO / VLSFO	Le Berre et al. (2024)
NO_X	51 ± 9	HFO / MDO	Celik et al. (2020)
	51–64	ULSD	Betha et al. (2016)
	64.5	MGO	Winnes et al. (2016)
	37 (28–48)	Mixed fuels	Le Berre et al. (2024)
	22.3 (median)	MDO (50 % load)	Zhang et al. (2024)
CO	20 ± 3	VLSFO / LSHFO / MDO	Celik et al. (2020)
	4–11.7	ULSD	Betha et al. (2016)
	5.4 (1.3–9.3)	Mixed fuels	Le Berre et al. (2024)
	↑ at low load	MGO / MDO	Bai et al. (2020)
CH_4	0.02	MDO	Cooper (2003)
	0.05	MGO (0.1 % S)	Timonen et al. (2022)
	0.4 (median)	Mixed fuels	Le Berre et al. (2024)
	0.99 (median)	MDO / MGO	Volent et al. (2025)
	5.2	Small vessels (gasoline)	Wang et al. (2022)
BC	0.9 ± 0.3	HFO / MDO	Celik et al. (2020)
	0.15 ± 0.17	HFO / MDO	Diesch et al. (2013)
	0.163–0.592	Mixed fuels	Le Berre et al. (2024)
	0.48	Cargo vessel (diesel)	Huang et al. (2018)
Org	3.0	HFO / MDO	Celik et al. (2020)
	1.8 ± 1.7	HFO / MDO	Diesch et al. (2013)
	0.86 (0.54–1.74)	Mixed fuels	Le Berre et al. (2024)
PAHs ($mg\ kg_{fuel}^{-1}$)	11	HFO / MDO	Celik et al. (2020)
	5.3	MDO	Diesch et al. (2013)
SO_4^{2-}	4 ± 1	HFO / MDO	Celik et al. (2020)
	0.54 ± 0.46	HFO / MDO	Diesch et al. (2013)
	0.05 (0.03–0.17)	Low-S fuels	Le Berre et al. (2024)
PN ($part\ kg_{fuel}^{-1}$)	1.2×10^{16} ($\pm3\times10^{15}$)	HFO / MDO	Celik et al. (2020)
	2.5×10^{16} (1.9×10^{16})	HFO / MDO	Diesch et al. (2013)
	8×10^{15}–1.1×10^{16}	ULSD	Betha et al. (2016)
	6.7×10^{15} (4.2–10.8×10^{15})	Mixed fuels	Le Berre et al. (2024)

S2 Positive Matrix Factorization (PMF) supporting analysis

S2.1 Input matrix and constrained factors

Table S6. Ions in constrained factors.

m/z	Molecular formula	Family Species	Shipping	COA	HOA
12	C	Cx	YES	YES	YES
13.0078201	CH	CH	YES	YES	YES
15.0234699	CH3	CH	YES	YES	YES
15.9949198	O	Air	YES	YES	YES
17.0027409	HO	HO	YES	YES	YES
18.0105591	H2O	HO	YES	YES	YES
21.9949207	CO2plus2	CHOgt1	YES	YES	YES
24	C2	Cx	YES	YES	YES
25.0078297	C2H	CH	YES	YES	YES
26.0156498	C2H2	CH	YES	YES	YES
27.0234795	C2H3	CH	YES	YES	YES
27.9949207	CO	CHO1	YES	YES	YES
29.0027409	CHO	CHO1	YES	YES	X
29.0391293	C2H5	CH	YES	YES	YES
30.0105591	CH2O	CHO1	YES	YES	X
30.0469494	C2H6	CH	YES	YES	YES
31.0183907	CH3O	CHO1	YES	YES	YES
36	C3	Cx	YES	X	YES
37.0078201	C3H	CH	YES	YES	YES
38.0156517	C3H2	CH	YES	YES	YES
39.0234795	C3H3	CH	YES	YES	YES
40.0312996	C3H4	CH	YES	YES	YES
41.002739	C2HO	CHO1	YES	YES	YES
41.0391197	C3H5	CH	YES	YES	YES
42.0105591	C2H2O	CHO1	YES	YES	YES
42.0469513	C3H6	CH	YES	YES	YES
43.0183907	C2H3O	CHO1	YES	YES	YES
43.0547791	C3H7	CH	YES	YES	YES
43.98983	CO2	CHOgt1	YES	YES	YES

Continuation of Table S6

m/z	Molecular formula	Family Species	Shipping	COA	HOA
44.0625992	C3H8	CH	YES	YES	YES
44.9976502	CHO2	CHOgt1	YES	YES	YES
45.0340385	C2H5O	CHO1	YES	YES	YES
46.0418701	C2H6O	CHO1	YES	X	YES
46.9688492	CCl	Cx	YES	X	X
49.0078201	C4H	CH	YES	YES	YES
50.0156517	C4H2	CH	YES	YES	YES
51.0234795	C4H3	CH	YES	YES	YES
52.0312996	C4H4	CH	YES	YES	YES
53.002739	C3HO	CHO1	YES	YES	YES
53.0391197	C4H5	CH	YES	YES	YES
54.0469513	C4H6	CH	YES	YES	YES
55.0183907	C3H3O	CHO1	YES	YES	YES
55.0547791	C4H7	CH	YES	YES	YES
56.0262108	C3H4O	CHO1	YES	YES	YES
56.0625992	C4H8	CH	YES	YES	YES
57.0340385	C3H5O	CHO1	YES	YES	YES
57.0704308	C4H9	CH	YES	YES	YES
58.0418701	C3H6O	CHO1	YES	YES	YES
58.0782509	C4H10	CH	YES	YES	YES
59.0133095	C2H3O2	CHOgt1	YES	YES	YES
59.0496903	C3H7O	CHO1	YES	YES	YES
59.0860754	C4H11	CH	YES	X	X
60.0211296	C2H4O2	CHOgt1	YES	YES	YES
61.0078201	C5H	CH	YES	YES	YES
61.0289497	C2H5O2	CHOgt1	YES	YES	YES
62.0156517	C5H2	CH	YES	YES	YES
63.0234795	C5H3	CH	YES	YES	YES
64.0313034	C5H4	CH	YES	YES	YES
65.0391235	C5H5	CH	YES	YES	YES
66.0469513	C5H6	CH	YES	YES	YES
67.0547714	C5H7	CH	YES	YES	YES
68.0625992	C5H8	CH	YES	YES	YES

Continuation of Table S6

m/z	Molecular formula	Family Species	Shipping	COA	HOA
69.0704269	C5H9	CH	YES	YES	YES
70.0418625	C4H6O	CHO1	YES	YES	YES
70.0782471	C5H10	CH	YES	YES	YES
71.0496903	C4H7O	CHO1	YES	YES	YES
71.0860672	C5H11	CH	YES	YES	YES
72.0211334	C3H4O2	CHOgt1	YES	YES	YES
72.057518	C4H8O	CHO1	YES	YES	YES
72.0939026	C5H12	CH	YES	YES	YES
73.0078278	C6H	CH	YES	X	YES
73.0653381	C4H9O	CHO1	YES	YES	YES
74.0156479	C6H2	CH	YES	YES	YES
74.0367813	C3H6O2	CHOgt1	YES	YES	YES
75.0234833	C6H3	CH	YES	YES	YES
76.0313034	C6H4	CH	YES	YES	YES
77.0391235	C6H5	CH	YES	YES	YES
78.0469513	C6H6	CH	YES	YES	YES
79.0547714	C6H7	CH	YES	YES	YES
80.062599	C6H8	CH	YES	YES	YES
81.070427	C6H9	CH	YES	YES	YES
82.041862	C5H6O	CHO1	YES	YES	YES
82.078247	C6H10	CH	YES	YES	YES
83.04969	C5H7O	CHO1	YES	YES	YES
83.086067	C6H11	CH	YES	YES	YES
84.057518	C5H8O	CHO1	YES	YES	YES
84.093903	C6H12	CH	YES	YES	YES
85.065338	C5H9O	CHO1	YES	YES	YES
85.101723	C6H13	CH	YES	YES	YES
86.0242	C3H4NO2	CHOgt1N	YES	X	X
86.048012	C3H6N2O	CHO1N	YES	X	X
86.073174	C5H10O	CHO1	YES	YES	YES
86.10955	C6H14	CH	YES	YES	YES
87.023483	C7H3	CH	YES	X	YES
87.080994	C5H11O	CHO1	YES	YES	YES

Continuation of Table S6

m/z	Molecular formula	Family Species	Shipping	COA	HOA
88.031303	C7H4	CH	YES	YES	YES
88.052429	C4H8O2	CHOgt1	YES	YES	YES
88.088814	C5H12O	CHO1	YES	YES	YES
89.039124	C7H5	CH	YES	YES	YES
90.046951	C7H6	CH	YES	YES	YES
91.054771	C7H7	CH	YES	YES	YES
92.062599	C7H8	CH	YES	YES	YES
93.070427	C7H9	CH	YES	YES	YES
94.041862	C6H6O	CHO1	YES	YES	YES
94.078247	C7H10	CH	YES	YES	YES
95.04969	C6H7O	CHO1	YES	YES	YES
95.086067	C7H11	CH	YES	YES	YES
96.057518	C6H8O	CHO1	YES	YES	YES
96.093903	C7H12	CH	YES	YES	YES
97.065338	C6H9O	CHO1	YES	YES	YES
97.101723	C7H13	CH	YES	YES	YES
98.015648	C8H2	CH	YES	X	YES
98.073174	C6H10O	CHO1	YES	YES	YES
98.10955	C7H14	CH	YES	YES	YES
99.023483	C8H3	CH	YES	X	YES
99.044601	C5H7O2	CHOgt1	YES	YES	YES
99.080994	C6H11O	CHO1	YES	YES	YES
99.117378	C7H15	CH	YES	YES	YES
100.031303	C8H4	CH	YES	X	YES
100.088799	C6H12O	CHO1	YES	YES	YES
100.125198	C7H16	CH	YES	X	YES
101.039101	C8H5	CH	YES	X	YES
101.096603	C6H13O	CHO1	YES	YES	YES
101.133026	C7H17	CH	YES	X	X
102.046997	C8H6	CH	YES	YES	YES
103.054802	C8H7	CH	YES	YES	YES
104.062599	C8H8	CH	YES	YES	YES
105.070396	C8H9	CH	YES	YES	YES

Continuation of Table S6

m/z	Molecular formula	Family Species	Shipping	COA	HOA
106.078201	C8H10	CH	YES	YES	YES
107.086098	C8H11	CH	YES	YES	YES
108.057503	C7H8O	CHO1	YES	X	YES
108.093903	C8H12	CH	YES	YES	YES
109.1017	C8H13	CH	YES	YES	YES
110.015602	C9H2	CH	YES	X	YES
110.073196	C7H10O	CHO1	YES	YES	YES
110.109596	C8H14	CH	YES	YES	YES
111.023499	C9H3	CH	YES	X	YES
111.081001	C7H11O	CHO1	YES	YES	YES
111.117401	C8H15	CH	YES	YES	YES
112.031303	C9H4	CH	YES	X	YES
112.088799	C7H12O	CHO1	YES	YES	YES
112.125198	C8H16	CH	YES	YES	YES
113.039101	C9H5	CH	YES	X	YES
113.096603	C7H13O	CHO1	YES	YES	YES
113.133003	C8H17	CH	YES	X	YES
114.046997	C9H6	CH	YES	X	YES
114.1045	C7H14O	CHO1	YES	YES	YES
114.1409	C8H18	CH	YES	YES	YES
115.054802	C9H7	CH	YES	YES	YES
115.112297	C7H15O	CHO1	YES	YES	YES
116.062599	C9H8	CH	YES	X	YES
117.070396	C9H9	CH	YES	X	YES
118.078201	C9H10	CH	YES	X	YES
119.049698	C8H7O	CHO1	YES	X	YES
119.086098	C9H11	CH	YES	X	YES
120.057503	C8H8O	CHO1	YES	X	YES
120.093903	C9H12	CH	YES	X	YES
121.0653	C8H9O	CHO1	YES	X	YES
121.1017	C9H13	CH	YES	X	YES
122.073196	C8H10O	CHO1	YES	X	YES
122.109596	C9H14	CH	YES	X	YES

Continuation of Table S6

m/z	Molecular formula	Family Species	Shipping	COA	HOA
123.081001	C8H11O	CHO1	YES	X	YES
123.117401	C9H15	CH	YES	X	YES
124.088799	C8H12O	CHO1	YES	X	YES
124.125198	C9H16	CH	YES	X	YES
125.096603	C8H13O	CHO1	YES	X	YES
125.133003	C9H17	CH	YES	X	YES
126.046997	C10H6	CH	YES	X	YES
126.1045	C8H14O	CHO1	YES	X	YES
126.1409	C9H18	CH	YES	X	YES
127.054802	C10H7	UnSubPAH	YES	X	YES
127.112297	C8H15O	CHO1	YES	X	YES
127.148697	C9H19	CH	YES	X	YES
128.062607	C10H8	UnSubPAH	YES	X	YES
128.071198	C6H10NO2	CHOgt1N	YES	X	X
128.083694	C7H12O2	CHOgt1	YES	X	YES
129.033997	C9H5O	CHO1	YES	X	X
129.070404	C10H9	CH	YES	X	YES
130.041901	C9H6O	CHO1	YES	X	YES
130.078201	C10H10	CH	YES	X	YES
131.049698	C9H7O	OPAH	YES	X	YES
131.086105	C10H11	CH	YES	X	YES
132.057495	C9H8O	OPAH	YES	X	X
132.093903	C10H12	CH	YES	X	X
133.065308	C9H9O	CHO1	YES	X	X
133.1017	C10H13	CH	YES	X	X
134.073196	C9H10O	CHO1	YES	X	X
134.109497	C10H14	CH	YES	X	X
135.080994	C9H11O	CHO1	YES	X	YES
135.117401	C10H15	CH	YES	X	YES
136.088806	C9H12O	CHO1	YES	X	YES
136.125198	C10H16	CH	YES	X	YES
137.096603	C9H13O	CHO1	YES	X	YES
137.132996	C10H17	CH	YES	X	YES

Continuation of Table S6

m/z	Molecular formula	Family Species	Shipping	COA	HOA
138.046997	C11H6	CH	YES	X	YES
138.104507	C9H14O	CHO1	YES	X	YES
138.1409	C10H18	CH	YES	X	YES
139.054794	C11H7	CH	YES	X	X
139.112305	C9H15O	CHO1	YES	X	YES
139.148697	C10H19	CH	YES	X	YES
140.062607	C11H8	CH	YES	X	X
140.120102	C9H16O	CHO1	YES	X	YES
140.156494	C10H20	CH	YES	X	YES
141.070404	C11H9	MPAH	YES	X	YES
141.164307	C10H21	CH	YES	X	YES
142.078201	C11H10	MPAH	YES	X	YES
142.172104	C10H22	CH	YES	X	X
143.049698	C10H7O	CHO1	YES	X	YES
143.086105	C11H11	CH	YES	X	YES
144.057495	C10H8O	CHO1	YES	X	YES
144.093903	C11H12	CH	YES	X	YES
145.065308	C10H9O	CHO1	YES	X	YES
145.1017	C11H13	CH	YES	X	YES
146.073196	C10H10O	CHO1	YES	X	YES
146.109497	C11H14	CH	YES	X	YES
147.053207	C5H9NO4	CHOgt1N	YES	X	X
147.080994	C10H11O	CHO1	YES	X	YES
147.117401	C11H15	CH	YES	X	YES
148.037201	C5H8O5	CHOgt1	YES	X	X
148.125198	C11H16	CH	YES	X	YES
149.044998	C5H9O5	CHOgt1	YES	X	YES
149.096603	C10H13O	CHO1	YES	X	YES
149.12	C10H15N	CHN	YES	X	X
151.054794	C12H7	UnSubPAH	YES	X	X
152.062607	C12H8	UnSubPAH	YES	X	YES
153.070404	C12H9	UnSubPAH	YES	X	YES
154.078201	C12H10	UnSubPAH	YES	X	YES

Continuation of Table S6

m/z	Molecular formula	Family Species	Shipping	COA	HOA
155.04969	C11H7O	OPAH	YES	X	X
155.086105	C12H11	MPAH	YES	X	YES
156.057515	C11H8O	OPAH	YES	X	X
156.093903	C12H12	MPAH	YES	X	YES
157.028954	C10H5O2	OPAH	YES	X	X
158.036804	C10H6O2	OPAH	YES	X	YES
165.070404	C13H9	UnSubPAH	YES	X	YES
166.078201	C13H10	UnSubPAH	YES	X	YES
167.04969	C12H7O	OPAH	YES	X	X
167.086105	C13H11	MPAH	YES	X	X
168.057515	C12H8O	OPAH	YES	X	X
168.093903	C13H12	MPAH	YES	X	YES
175.054775	C14H7	UnSubPAH	YES	X	X
176.062607	C14H8	UnSubPAH	YES	X	X
177.070404	C14H9	UnSubPAH	YES	X	X
178.078201	C14H10	UnSubPAH	YES	X	YES
179.04969	C13H7O	OPAH	YES	X	X
179.086105	C14H11	MPAH	YES	X	YES
180.057515	C13H8O	OPAH	YES	X	X
180.093903	C14H12	MPAH	YES	X	YES
181.028954	C12H5O2	OPAH	YES	X	X
181.06534	C13H9O	OPAH	YES	X	X
182.036779	C12H6O2	OPAH	YES	X	X
183.044605	C12H7O2	OPAH	YES	X	X
189.070404	C15H9	UnSubPAH	YES	X	YES
190.078201	C15H10	UnSubPAH	YES	X	YES
191.086105	C15H11	MPAH	YES	X	YES
192.093903	C15H12	MPAH	YES	X	X
193.06534	C14H9O	OPAH	YES	X	X
194.073196	C14H10O	OPAH	YES	X	YES
194.109497	C15H14	MPAH	YES	X	YES
195.044605	C13H7O2	OPAH	YES	X	X
196.05243	C13H8O2	OPAH	YES	X	X

Continuation of Table S6

m/z	Molecular formula	Family Species	Shipping	COA	HOA
201.070425	C16H9	UnSubPAH	YES	X	X
202.078201	C16H10	UnSubPAH	YES	X	YES
203.04969	C15H7O	OPAH	YES	X	X
204.057515	C15H8O	OPAH	YES	X	X
205.101725	C16H13	MPAH	YES	X	X
206.109497	C16H14	MPAH	YES	X	X
207.044605	C14H7O2	OPAH	YES	X	X
208.05243	C14H8O2	OPAH	YES	X	X
215.086075	C17H11	UnSubPAH	YES	X	X
216.0939	C17H12	UnSubPAH	YES	X	X
219.117376	C17H15	MPAH	YES	X	X
220.125201	C17H16	MPAH	YES	X	X
225.070425	C18H9	UnSubPAH	YES	X	X
226.07825	C18H10	UnSubPAH	YES	X	X
227.086075	C18H11	UnSubPAH	YES	X	X
228.0939	C18H12	UnSubPAH	YES	X	X
231.044605	C16H7O2	OPAH	YES	X	X
232.05243	C16H8O2	OPAH	YES	X	X
233.133026	C18H17	MPAH	YES	X	X
234.140851	C18H18	MPAH	YES	X	X
241.101725	C19H13	MPAH	YES	X	X
249.070425	C20H9	UnSubPAH	YES	X	X
250.07825	C20H10	UnSubPAH	YES	X	X
251.086075	C20H11	UnSubPAH	YES	X	X
252.0939	C20H12	UnSubPAH	YES	X	X
253.06534	C19H9O	OPAH	YES	X	X
254.073165	C19H10O	OPAH	YES	X	X
255.117376	C20H15	MPAH	YES	X	X
256.125201	C20H16	MPAH	YES	X	X

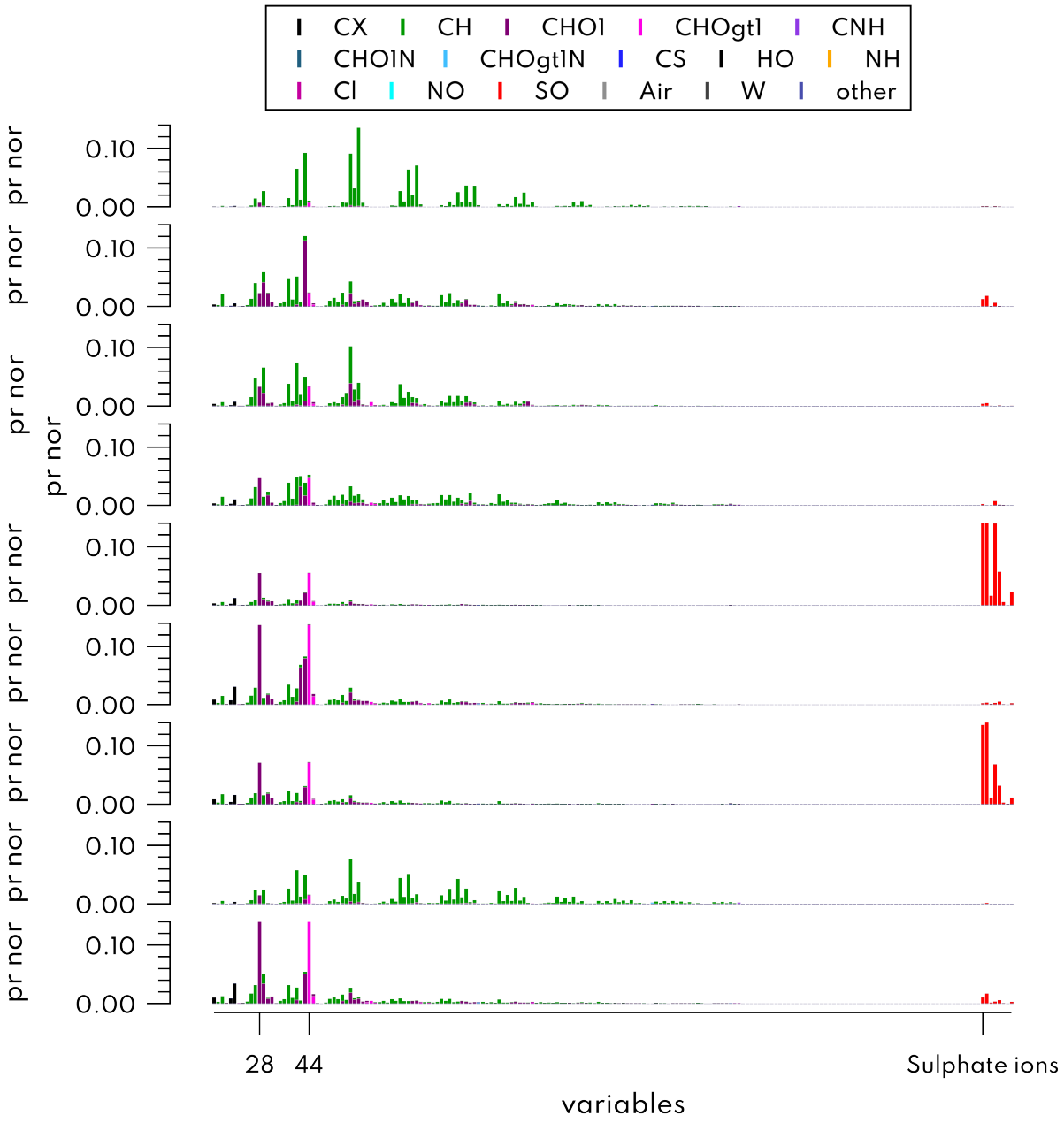

Figure S7. Mass spectra of the 9-factors PMF solution with sulfate ions added.

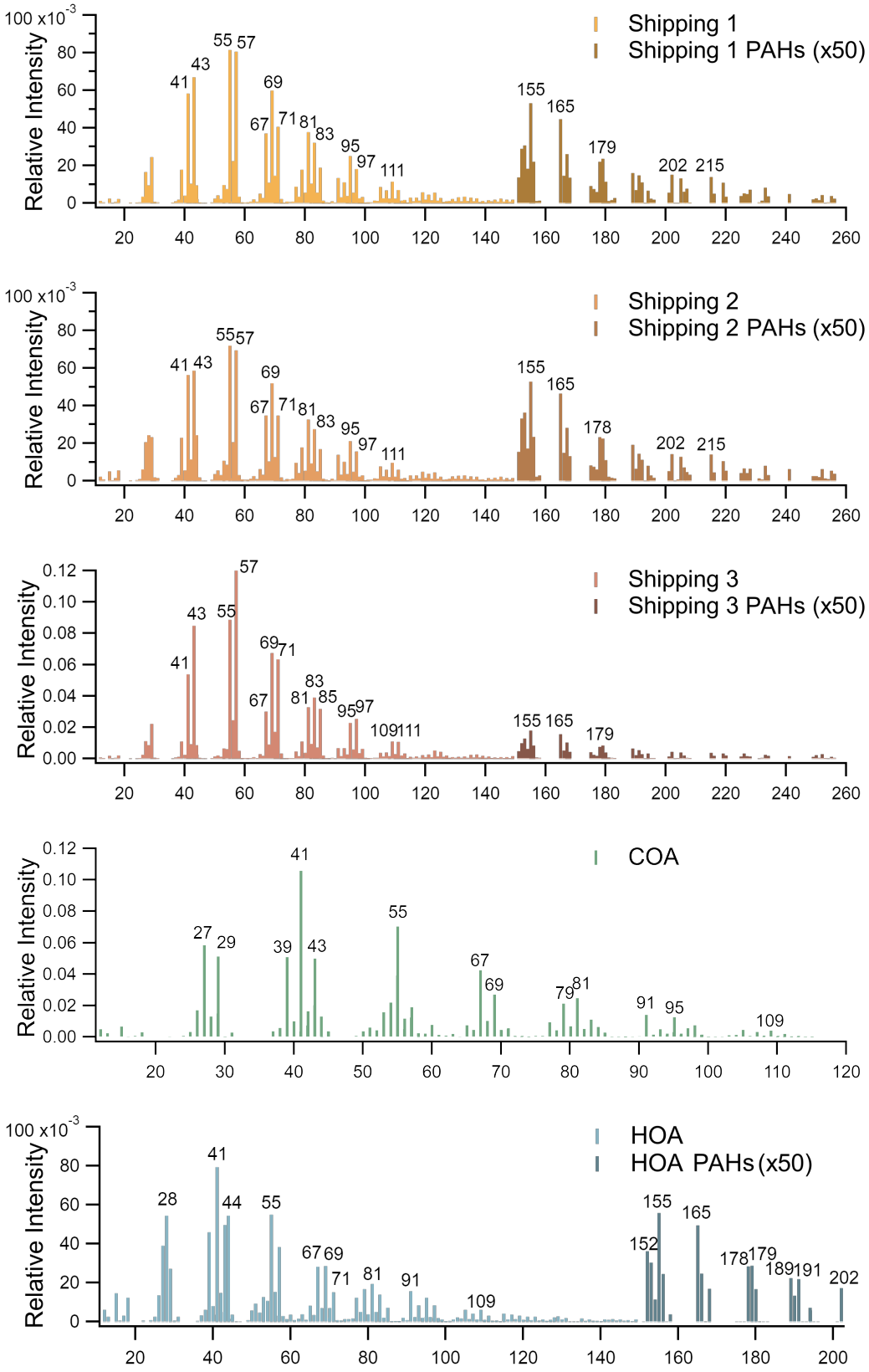

Figure S8. Reference mass spectra used as constraints for PMF analysis. Ions with *m/z* ratio superior to 150 have their relative intensity multiplied by 50 to enhance readability. X-axis represents *m/z* ratios.

S2.2 Residuals, error estimation and bootstrap validation

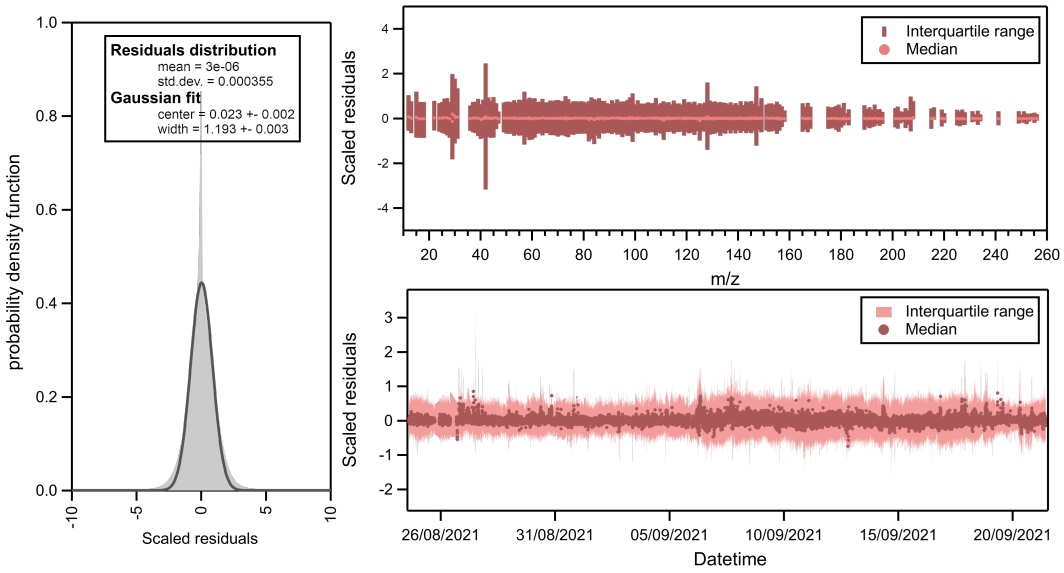

Figure S9. Scaled residuals distribution fitted by a Gaussian curve (a). Median scaled and interquartile range for the solution over m/z profile (a) and time (b).

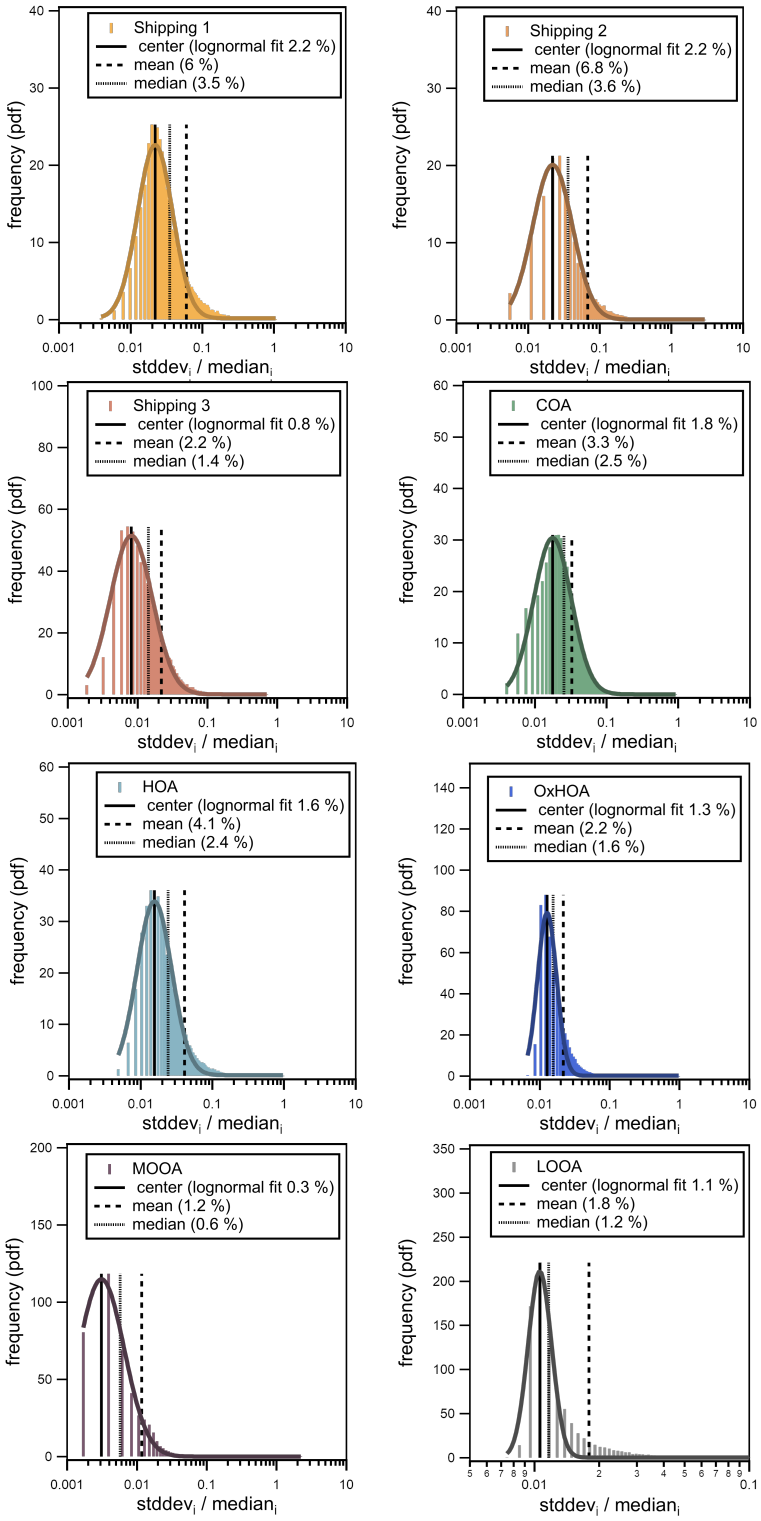

Figure S10. PMF error estimation for each factors, the center of the lognormal fit corresponds to the uncertainties of the factor.

S2.3 Spectral similarity and SRP analyses

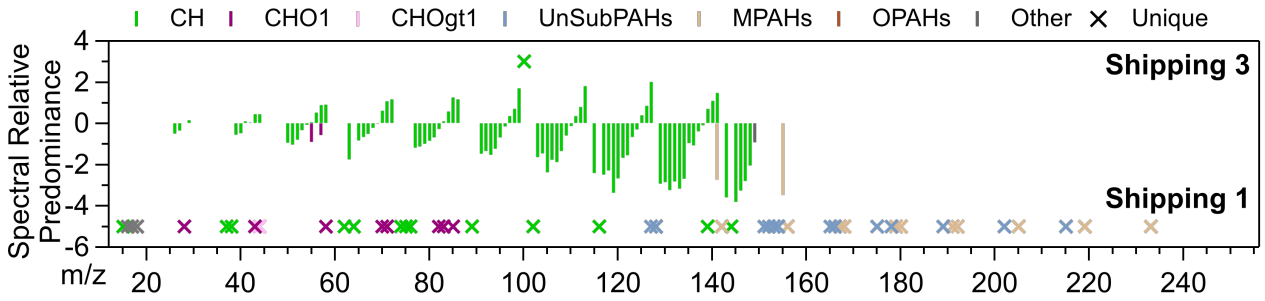

Figure S11. Spectral Relative Predominance (SRP) of Shipping 3 factor (positives SRP) with Shipping 1 factor (negatives SRP). Ions whose intensity are below their median error are considered zero. Cross markers represents ions that are null intensity in the other factor. Ions are family-colored.

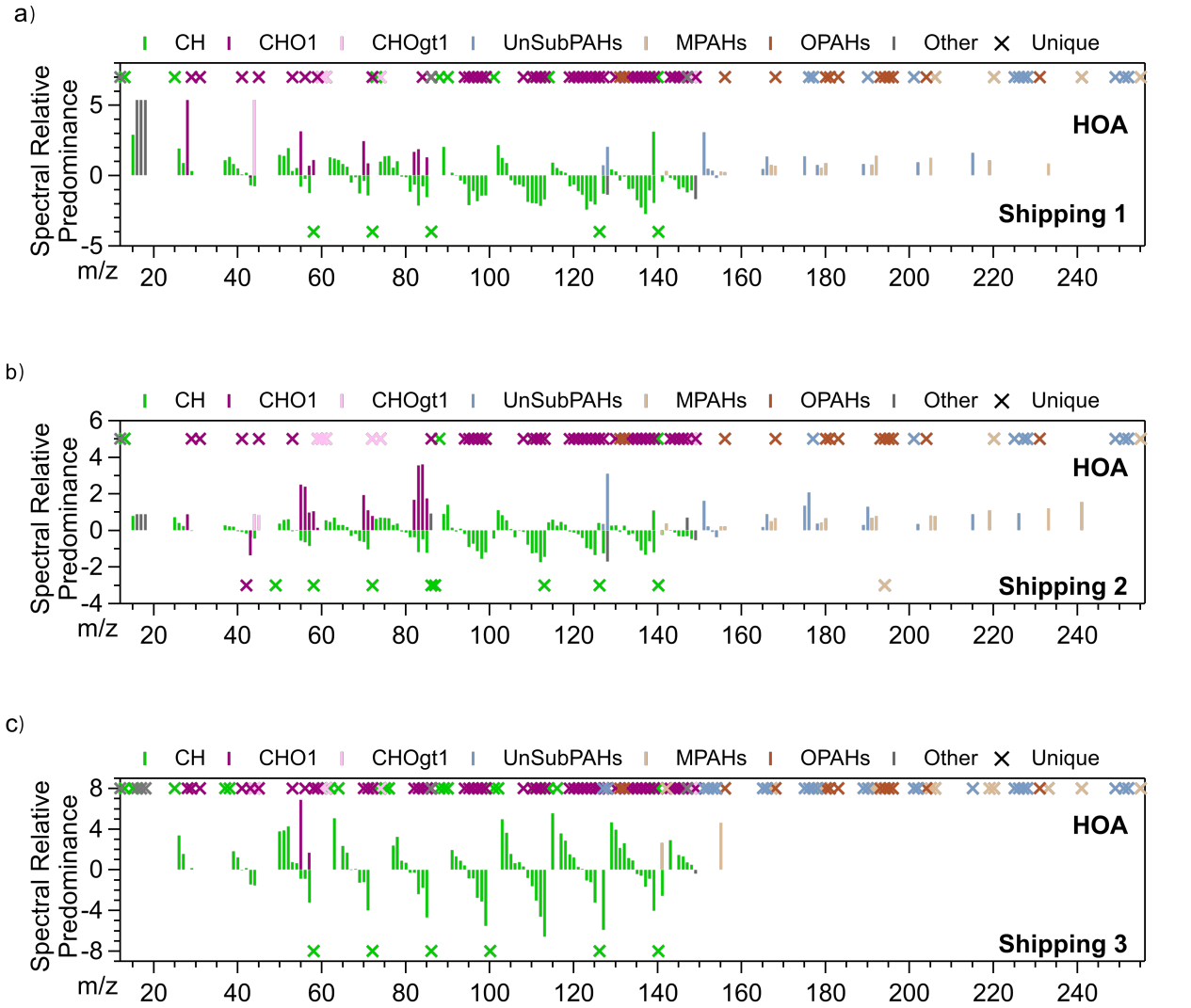

Figure S12. Spectral Relative Predominance (SRP) of HOA factor (positives SRP) with shipping factors 1 (a)), 2 (b)) and 3 (c)) (negatives SRP). Ions whose intensity are below their median error are considered zero. Cross markers represents ions that are null intensity in the other factor. Ions are family-colored.

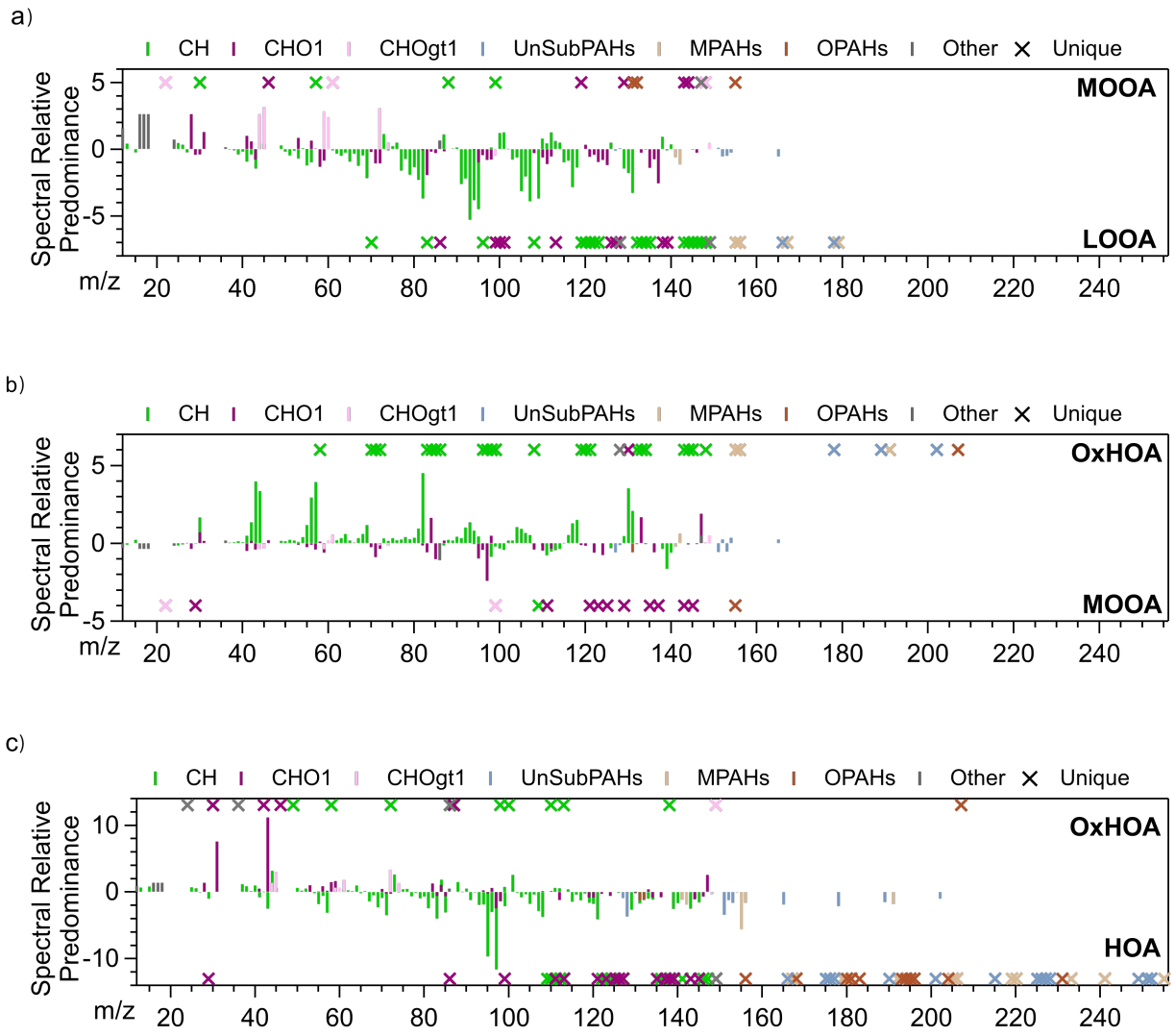

Figure S13. Spectral Relative Predominance (SRP) of MOOA factor (positives SRP) with LOOA factor (negatives SRP) (a)) and OxHOA factor (positives SRP) with MOOA (b)) and HOA factors (c))(negatives SRP). Ions whose intensity are below their median error are considered zero. Cross markers represents ions that are null intensity in the other factor. Ions are family-colored.

S2.4 Factor–tracer correlations and wind dependence

Table S7. Hourly R Pearson correlation between factors and instruments time series. Bold numbers represent noticeable correlations.

R Pearson	Shipping 1	Shipping 2	Shipping 3	COA	HOA	OxHOA	MOOA	LOOA
SO_2	**0.26**	**0.34**	0.06	-0.18	-0.12	-0.08	-0.08	-0.17
BC	**0.37**	**0.56**	**0.40**	0.09	**0.26**	**0.39**	-0.06	0.18
CO	0.12	0.27	0.43	**0.39**	**0.51**	**0.64**	-0.04	0.32
CO_2	0.07	0.09	0.20	0.24	**0.31**	**0.48**	-0.11	**0.54**
CH_4	-0.10	-0.12	0.01	0.08	0.12	0.14	0.07	0.08
NO_x	**0.54**	**0.73**	**0.52**	0.11	**0.28**	**0.37**	-0.17	0.06
O_3	-0.23	-0.32	-0.28	-0.25	-0.31	-0.56	0.48	-0.55
Wind dir	0.13	0.16	0.11	0.00	0.00	0.07	-0.12	0.03
Wind vel	0.35	0.34	0.05	-0.34	-0.34	-0.46	-0.12	-0.39
$N_{15nm-30nm}$	**0.59**	**0.69**	0.11	0.01	0.07	0.08	-0.18	0.00
$N_{30nm-50nm}$	**0.71**	**0.75**	0.16	0.08	0.09	0.11	-0.17	0.02
$N_{50nm-70nm}$	**0.77**	**0.78**	0.20	0.13	0.15	0.16	-0.17	0.09
$N_{70nm-100nm}$	0.46	0.53	0.23	0.26	**0.34**	**0.33**	-0.10	**0.31**
$N_{100nm-200nm}$	0.16	0.22	**0.30**	**0.35**	**0.45**	**0.50**	0.22	**0.43**
$N_{200nm-661nm}$	0.05	0.04	0.12	0.11	0.17	**0.32**	**0.24**	0.10
Org	0.45	0.41	0.44	0.57	0.55	0.58	0.42	0.61
NO_3^-	-0.04	-0.05	0.17	0.55	0.57	**0.7**	0.34	**0.79**
SO_4^{2-}	-0.1	-0.17	0.03	0.14	0.05	**0.43**	**0.51**	0
NH_4^+	-0.13	-0.19	0.04	0.17	0.06	**0.5**	**0.46**	0.06

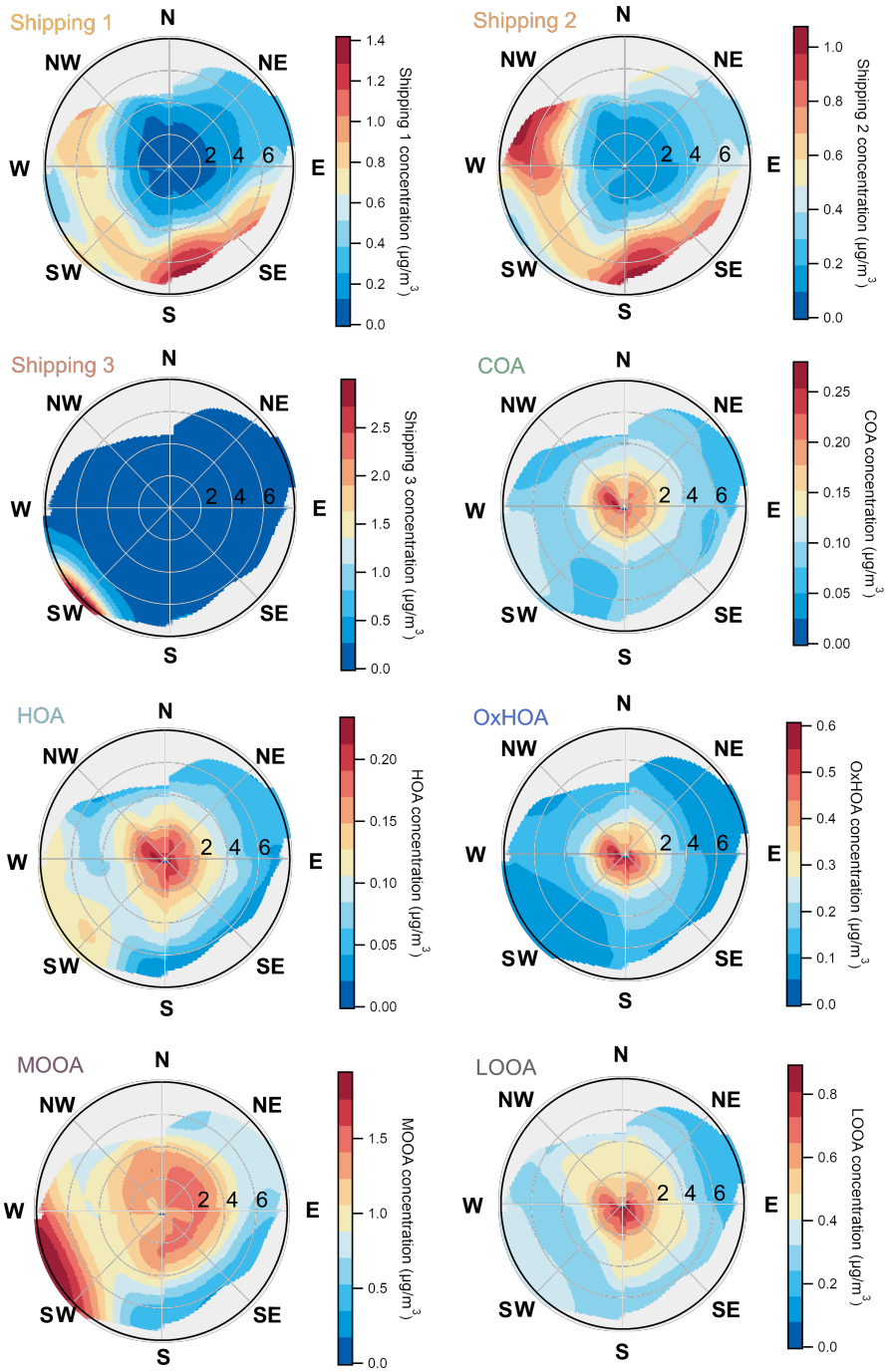

Figure S14. Non-parametric wind regression (NWR) plot of PMF factors, x-axis indicates wind intensity in m/s.

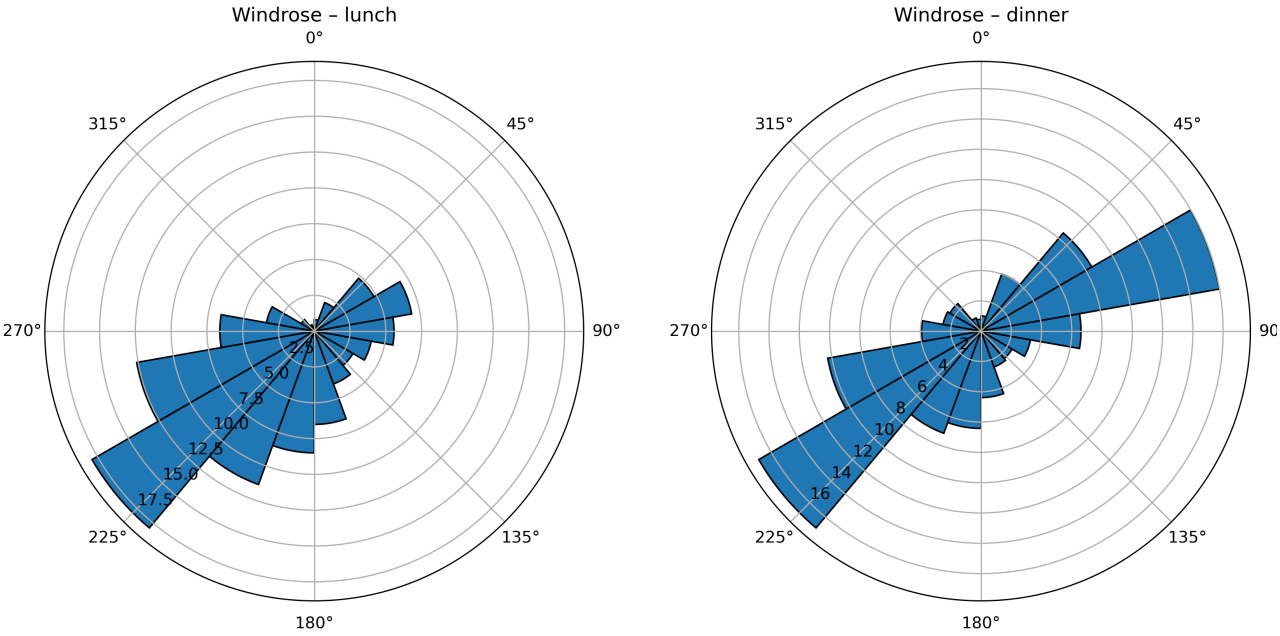

Figure S15. Wind roses during meal-time periods (a) lunch, 11:00–14:00, and (b) dinner, 18:00–21:00, over the entire campaign. The restaurant areas are located to the north–northwest of the site (315°–360° sector). Only 0.78 % (lunch) and 2.05 % (dinner) of winds originated from this direction, indicating that the site was rarely downwind of potential cooking sources during these periods.

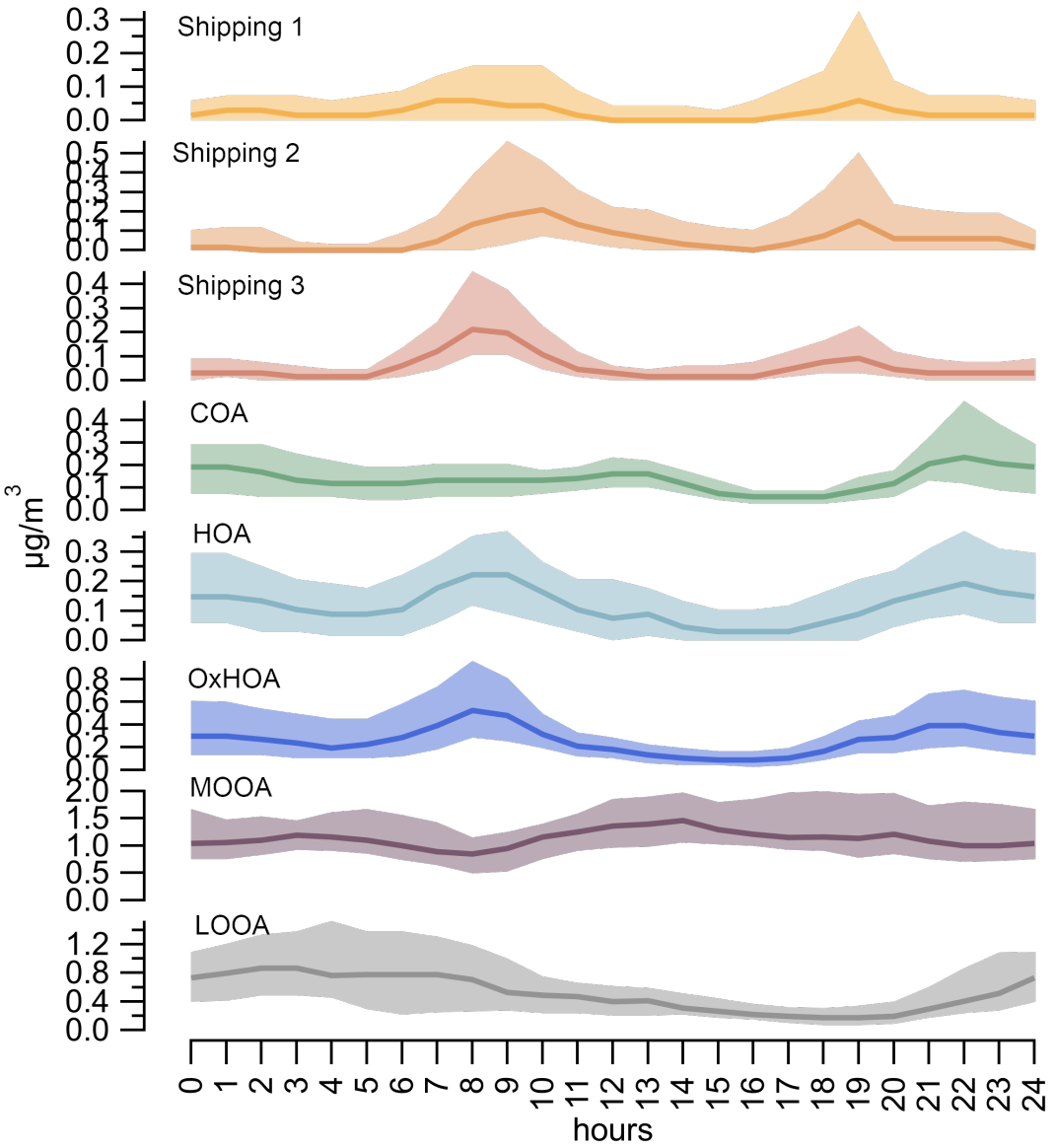

Figure S16. Diurnal variation of the PMF factors.

Table S8. Cosine similarities between PMF factors.

	Shipping 1	Shipping 2	Shipping 3	COA	HOA	OxHOA	MOOA	LOOA
Shipping 1	1.00	0.96	0.93	0.79	0.79	0.31	0.18	0.37
Shipping 2	0.96	1.00	0.90	0.87	0.91	0.51	0.37	0.52
Shipping 3	0.93	0.90	1.00	0.67	0.69	0.24	0.13	0.25
COA	0.79	0.87	0.67	1.00	0.87	0.47	0.34	0.62
HOA	0.79	0.91	0.69	0.87	1.00	0.73	0.63	0.67
OxHOA	0.31	0.51	0.24	0.47	0.73	1.00	0.98	0.75
MOOA	0.18	0.37	0.13	0.34	0.63	0.98	1.00	0.70
LOOA	0.37	0.52	0.25	0.62	0.67	0.75	0.70	1.00

S2.5 Chemical characterization and interpretation

Table S9. O:C, H:C and OM:OC ratio, calculated with APES Light code, based on the work of Aiken et al. (2007, 2008), for all ions and for ions with m/z inferior to 120.

	all m/z			m/z <120		
	O:C	H:C	OM:OC	O:C	H:C	OM:OC
Shipping 1	0.02	1.87	1.29	0.03	1.99	1.21
Shipping 2	0.05	1.81	1.31	0.09	1.91	1.28
Shipping 3	0.01	2.15	1.31	0.02	2.21	1.22
COA	0.12	1.81	1.36	0.13	1.86	1.33
HOA	0.12	1.63	1.35	0.21	1.77	1.43
OxHOA	0.34	1.43	1.54	0.50	1.52	1.79
MOOA	0.52	1.28	1.69	0.72	1.28	2.08
LOOA	0.23	1.49	1.43	0.33	1.58	1.58

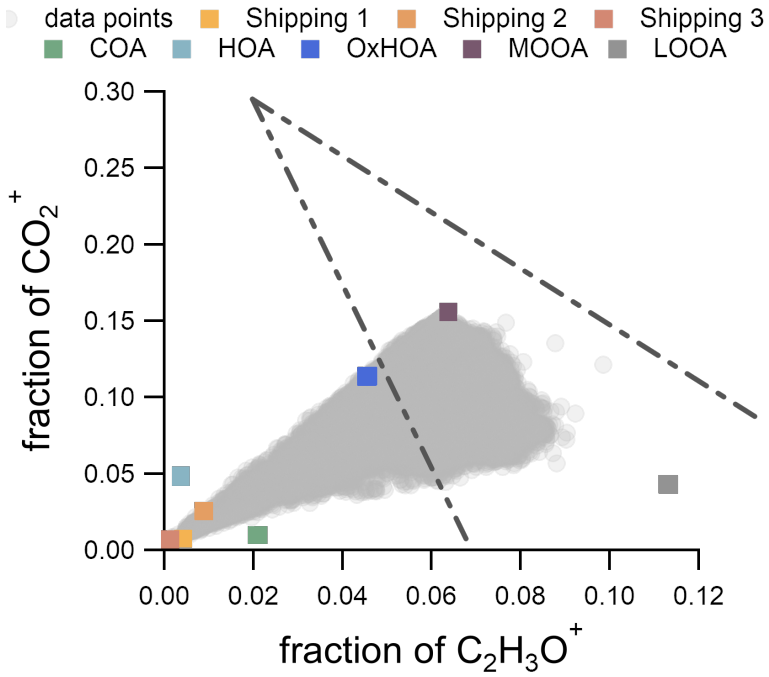

Figure S17. Fraction of CO_2^+ vs. fraction of $C_2H_3O^+$. Dashed lines represent the limits of Ng et al. (2010)'s triangle. Factors are substracted from total contribution.

Table S10. Correlation between Shipping 1 factor and top 5 (and oleic acid) correlated spectra from HR-AMS Database.

rank	$\cos\theta$	θ	Type / Compound	Location	Date	Reference
1	0.97	0.22	HOA	Riverside, CA, USA	July 2005	Docherty et al. (2011)
2	0.96	0.27	HOA	Barcelona, Spain	March 2009	Mohr et al. (2012)
3	0.96	0.30	HOA	Oakland, CA, USA	Summer 2017	Shah et al. (2018)
4	0.94	0.36	HOA	Xian and Beijing, China	Dec 2013-Jan 2014	Elser et al. (2016)
5	0.93	0.39	HOA	Mexico City, Mexico	March 2009	Aiken et al. (2009)
7	0.88	0.49	Oleic Acid	Laboratory		Hu et al. (2018)

Table S11. Correlation between Shipping 2 factor and top 5 correlated spectra from HR-AMS Database.

rank	$\cos\theta$	θ	Type	Location	Date	Reference
1	0.97	0.22	HOA	Beijing, China	Aug-Sep 2011	Hu et al. (2016)
2	0.96	0.27	HOA	Mexico City, Mexico	March 2009	Aiken et al. (2009)
3	0.96	0.30	HOA	Xian and Beijing, China	Dec 2013-Jan 2014	Elser et al. (2016)
4	0.94	0.36	HOA	Riverside, CA, USA	July 2005	Docherty et al. (2011)
5	0.93	0.39	HOA	Paris, France	Summer 2009	Crippa et al. (2013)

Table S12. Correlation between Shipping 3 factor and top 5 correlated spectra from HR-AMS Database.

rank	$\cos\theta$	θ	Type / Compound	Location	Date	Reference
1	0.98	0.20	HOA	Oakland, CA, USA	Summer 2017	Shah et al. (2018)
2	0.96	0.27	HOA	Barcelona, Spain	March 2009	Mohr et al. (2012)
3	0.96	0.28	HOA	Riverside, CA, USA	July 2005	Docherty et al. (2011)
4	0.92	0.39	Dioctyl selecate	Chamber		Hu et al. (2018)
5	0.92	0.40	HOA	Xian and Beijing, China	Dec 2013-Jan 2014	Elser et al. (2016)

Table S13. Correlation between COA factor and top 5 correlated spectra from HR-AMS Database.

rank	$\cos\theta$	θ	Type / Compound	Location	Date	Reference
1	0.99	0.15	COA	Paris, France	Summer 2009	Crippa et al. (2013)
2	0.99	0.16	COA	Xian and Beijing, China	Dec 2013-Jan 2014	Elser et al. (2016)
3	0.98	0.22	COA	Oakland, CA, USA	Summer 2017	Shah et al. (2018)
4	0.96	0.27	Oleic Acid (C18H34O2)			Hu et al. (2018)
5	0.96	0.28	COA	Rome, Italy	June 2014	Struckmeier et al. (2016)

Table S14. Correlation between HOA factor and top 5 correlated spectra from HR-AMS Database.

rank	$\cos\theta$	θ	Type	Location	Date	Reference
1	0.97	0.26	HOA	Pasadena, CA, USA	2010	Hayes et al. (2013)
2	0.96	0.3	COA	Beijing, China	Aug-Sep, 2011	Hu et al. (2016)
3	0.94	0.35	Ambient with strong Biomass Burning events and OA background removed	Changdao Island, China	March-April 2011	Hu et al. (2013)
4	0.94	0.36	HOA	Flight, South Korea	May 2006	Hu et al. (2018)
5	0.94	0.36	HOA	Station Po Valley, Italy	April 2008	Saarikoski et al. (2012)

Table S15. Correlation between OxHOA factor and top 5 correlated spectra from HR-AMS Database.

rank	$\cos\theta$	θ	Type	O:C ratio	Location	Date	Reference
1	0.98	0.22	MOOA	0.58	Beijing, China	Aug-Sep, 2011	Hu et al. (2016)
2	0.97	0.23	LOOA	0.42	Cool, CA, USA	June 2010	Setyan et al. (2012)
3	0.97	0.26	MOOA*	0.73	Paris, France	Summer 2009	Crippa et al. (2013)
4	0.97	0.26	OOAa**	0.74**	Station Po Valley, Italy	April 2008	Saarikoski et al. (2012)
5	0.97	0.26	OOAb**	0.74**	Station Po Valley, Italy	April 2008	Saarikoski et al. (2012)

*originally LV-OOA (Low-Volatility Oxygenated Organic Aerosol), corresponding to MOOA
** these OOA has been regroup as a single MOOA factor in Saarikoski et al. (2012), with a O/C ratio of 0.74

Table S16. Correlation between MOOA factor and top 5 correlated spectra from HR-AMS Database.

rank	$\cos\theta$	θ	Type	O:C ratio	Location	Date	Reference
1	0.99	0.12	OOAa	0.74	Station Po Valley, Italy	April 2008	Saarikoski et al. (2012)
2	0.99	0.13	MOOA		Centreville, AL, USA	June-July 2013	Hu et al. (2015)
3	0.99	0.14	MOOA*	0.72	Riverside, CA, USA	July 2005	Docherty et al. (2011)
4	0.99	0.15	MOOA	0.58	Beijing, China	Aug-Sep, 2011	Hu et al. (2016)
5	0.99	0.15	MOOA	1.12** 1.13***	Flight, South Korea	May 2006	Hu et al. (2018)

*originattely LV-OOA (Low-Volatility Oxygenated Organic Aerosol), corresponding to MOOA in this paper
** with standard vaporizer, *** with new capture vaporizer

Table S17. Correlation between LOOA factor and top 5 correlated spectra from HR-AMS Database.

rank	$\cos\theta$	θ	Type	O:C ratio	Location	Date	Reference
1	0.97	0.26	LOOA		Paris, France	Summer 2009	Crippa et al. (2013)
2	0.97	0.26	LOOA		Riverside, CA, USA	July 2005	Docherty et al. (2011)
3	0.96	0.28	LOOA		Flight, South Korea	May 2006	Hu et al. (2018)
4	0.96	0.29	LOOA	0.47	Beijing, China	Aug-Sep, 2011	Hu et al. (2016)
5	0.95	0.31	LOOA		Centreville, AL, USA	June-July 2013	Hu et al. (2015)

Table S18. Diurnal Pearson R correlation between PMF factors.

	Shipping 1	Shipping 2	Shipping 3	COA	HOA	OxHOA	MOOA	LOOA
Shipping 1	1.00	0.92	0.83	-0.35	0.15	0.19	-0.06	-0.54
Shipping 2	0.92	1.00	0.73	-0.18	0.24	0.19	-0.01	-0.60
Shipping 3	0.83	0.73	1.00	-0.30	0.35	0.45	-0.45	-0.15
COA	-0.35	-0.18	-0.30	1.00	0.72	0.59	-0.27	0.34
HOA	0.15	0.24	0.35	0.72	1.00	0.96	-0.74	0.41
OxHOA	0.19	0.19	0.45	0.59	0.96	1.00	-0.84	0.50
MOOA	-0.06	-0.01	-0.45	-0.27	-0.74	-0.84	1.00	-0.75
LOOA	-0.54	-0.60	-0.15	0.34	0.41	0.50	-0.75	1.00

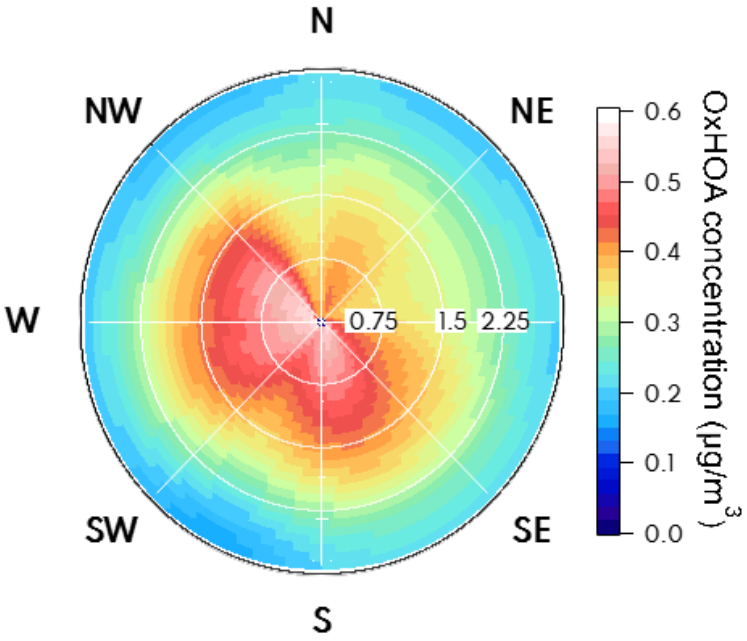

Figure S18. Non-parametric wind regression plot of OxHOA factor (zoomed), x-axis indicates wind intensity in m/s.

References

Aiken, A. C., DeCarlo, P. F., and Jimenez, J. L.: Elemental Analysis of Organic Species with Electron Ionization High-Resolution Mass Spectrometry, Analytical Chemistry, 79, 8350–8358, doi:10.1021/ac071150w, pMID: 17914892, 2007.

Aiken, A. C., DeCarlo, P. F., Kroll, J. H., Worsnop, D. R., Huffman, J. A., Docherty, K. S., Ulbrich, I. M., Mohr, C., Kimmel, J. R., Sueper, D., Sun, Y., Zhang, Q., Trimborn, A., Northway, M., Ziemann, P. J., Canagaratna, M. R., Onasch, T. B., Alfarra, M. R., Prevot, A. S. H., Dommen, J., Duplissy, J., Metzger, A., Baltensperger, U., and Jimenez, J. L.: O/C and OM/OC Ratios of Primary, Secondary, and Ambient Organic Aerosols with High-Resolution Time-of-Flight Aerosol Mass Spectrometry, Environmental Science & Technology, 42, 4478–4485, doi:10.1021/es703009q, pMID: 18605574, 2008.

Aiken, A. C., Salcedo, D., Cubison, M. J., Huffman, J. A., DeCarlo, P. F., Ulbrich, I. M., Docherty, K. S., Sueper, D., Kimmel, J. R., Worsnop, D. R., Trimborn, A., Northway, M., Stone, E. A., Schauer, J. J., Volkamer, R. M., Fortner, E., de Foy, B., Wang, J., Laskin, A., Shutthanandan, V., Zheng, J., Zhang, R., Gaffney, J., Marley, N. A., Paredes-Miranda, G., Arnott, W. P., Molina, L. T., Sosa, G., and Jimenez, J. L.: Mexico City aerosol analysis during MILAGRO using high resolution aerosol mass spectrometry at the urban supersite (T0) – Part 1: Fine particle composition and organic source apportionment, Atmospheric Chemistry and Physics, 9, 6633–6653, doi:10.5194/acp-9-6633-2009, 2009.

Bahreini, R., Ervens, B., Middlebrook, A. M., Warneke, C., de Gouw, J. A., DeCarlo, P. F., Jimenez, J. L., Brock, C. A., Neuman, J. A., Ryerson, T. B., Stark, H., Atlas, E., Brioude, J., Fried, A., Holloway, J. S., Peischl, J., Richter, D., Walega, J., Weibring, P., Wollny, A. G., and Fehsenfeld, F. C.: Organic aerosol formation in urban and industrial plumes near Houston and Dallas, Texas, Journal of Geophysical Research: Atmospheres, 114, doi:10.1029/2008JD011493, 2009.

Bai, C., Li, Y., Liu, B., Zhang, Z., and Wu, P.: Gaseous Emissions from a Seagoing Ship under Different Operating Conditions in the Coastal Region of China, Atmosphere, 11, doi:10.3390/atmos11030305, 2020.

Betha, R., Russell, L., Sanchez, K., Liu, J., Price, D., Lamjiri, M., Chen, C.-L., Kuang, X., Da Rocha, G., Paulson, S., Miller, J., and Cocker, D.: Lower NO x but Higher Particle and Black Carbon Emissions from Renewable Diesel compared to Ultra Low Sulfur Diesel in At-Sea Operations of a Research Vessel, Aerosol Science and Technology, 51, 00–00, doi:10.1080/02786826.2016.1238034, 2016.

Brendan M. Matthew, A. M. M. and Onasch, T. B.: Collection Efficiencies in an Aerodyne Aerosol Mass Spectrometer as a Function of Particle Phase for Laboratory Generated Aerosols, Aerosol Science and Technology, 42, 884–898, doi:10.1080/02786820802356797, 2008.

Canagaratna, M., Jayne, J., Jimenez, J., Allan, J., Alfarra, M., Zhang, Q., Onasch, T., Drewnick, F., Coe, H.,

Middlebrook, A., Delia, A., Williams, L., Trimborn, A., Northway, M., DeCarlo, P., Kolb, C., Davidovits, P., and Worsnop, D.: Chemical and microphysical characterization of ambient aerosols with the aerodyne aerosol mass spectrometer, Mass Spectrometry Reviews, 26, 185–222, doi:10.1002/mas.20115, 2007.

Celik, S., Drewnick, F., Fachinger, F., Brooks, J., Darbyshire, E., Coe, H., Paris, J.-D., Eger, P. G., Schuladen, J., Tadic, I., Friedrich, N., Dienhart, D., Hottmann, B., Fischer, H., Crowley, J. N., Harder, H., and Borrmann, S.: Influence of vessel characteristics and atmospheric processes on the gas and particle phase of ship emission plumes: in situ measurements in the Mediterranean Sea and around the Arabian Peninsula, Atmospheric Chemistry and Physics, 20, 4713–4734, doi:10.5194/acp-20-4713-2020, 2020.

Cooper, D.: Exhaust emissions from ships at berth, Atmospheric Environment, 37, 3817–3830, doi:10.1016/S1352-2310(03)00446-1, 2003.

Crippa, M., El Haddad, I., Slowik, J. G., DeCarlo, P. F., Mohr, C., Heringa, M. F., Chirico, R., Marchand, N., Sciare, J., Baltensperger, U., and Prévôt, A. S. H.: Identification of marine and continental aerosol sources in Paris using high resolution aerosol mass spectrometry, Journal of Geophysical Research: Atmospheres, 118, 1950–1963, doi:https://doi.org/10.1002/jgrd.50151, 2013.

DeCarlo, P. F., Kimmel, J. R., Trimborn, A., Northway, M. J., Jayne, J. T., Aiken, A. C., Gonin, M., Fuhrer, K., Horvath, T., Docherty, K. S., Worsnop, D. R., and Jimenez, J. L.: Field-Deployable, High-Resolution, Time-of-Flight Aerosol Mass Spectrometer, Analytical Chemistry, 78, 8281–8289, doi:10.1021/ac061249n, 2006.

Diesch, J.-M., Drewnick, F., Klimach, T., and Borrmann, S.: Investigation of gaseous and particulate emissions from various marine vessel types measured on the banks of the Elbe in Northern Germany, Atmospheric Chemistry and Physics, 13, 3603–3618, doi:10.5194/acp-13-3603-2013, 2013.

Docherty, K. S., Aiken, A. C., Huffman, J. A., Ulbrich, I. M., DeCarlo, P. F., Sueper, D., Worsnop, D. R., Snyder, D. C., Peltier, R. E., Weber, R. J., Grover, B. D., Eatough, D. J., Williams, B. J., Goldstein, A. H., Ziemann, P. J., and Jimenez, J. L.: The 2005 Study of Organic Aerosols at Riverside (SOAR-1): instrumental intercomparisons and fine particle composition, Atmospheric Chemistry and Physics, 11, 12 387–12 420, doi:10.5194/acp-11-12387-2011, 2011.

Elser, M., Bozzetti, C., El-Haddad, I., Maasikmets, M., Teinemaa, E., Richter, R., Wolf, R., Slowik, J. G., Baltensperger, U., and Prévôt, A. S. H.: Urban increments of gaseous and aerosol pollutants and their sources using mobile aerosol mass spectrometry measurements, Atmospheric Chemistry and Physics, 16, 7117–7134, doi:10.5194/acp-16-7117-2016, 2016.

Hayes, P. L., Ortega, A. M., Cubison, M. J., Froyd, K. D., Zhao, Y., Cliff, S. S., Hu, W. W., Toohey, D. W., Flynn, J. H., Lefer, B. L., Grossberg, N., Alvarez, S., Rappenglück, B., Taylor, J. W., Allan, J. D., Holloway, J. S., Gilman, J. B., Kuster, W. C., de Gouw, J. A., Massoli, P., Zhang, X., Liu, J., Weber, R. J., Corrigan,

A. L., Russell, L. M., Isaacman, G., Worton, D. R., Kreisberg, N. M., Goldstein, A. H., Thalman, R., Waxman, E. M., Volkamer, R., Lin, Y. H., Surratt, J. D., Kleindienst, T. E., Offenberg, J. H., Dusanter, S., Griffith, S., Stevens, P. S., Brioude, J., Angevine, W. M., and Jimenez, J. L.: Organic aerosol composition and sources in Pasadena, California, during the 2010 CalNex campaign, Journal of Geophysical Research: Atmospheres, 118, 9233–9257, doi:10.1002/jgrd.50530, 2013.

Hu, W., Hu, M., Hu, W., Jimenez, J. L., Yuan, B., Chen, W., Wang, M., Wu, Y., Chen, C., Wang, Z., Peng, J., Zeng, L., and Shao, M.: Chemical composition, sources, and aging process of submicron aerosols in Beijing: Contrast between summer and winter, Journal of Geophysical Research: Atmospheres, 121, 1955–1977, doi:https://doi.org/10.1002/2015JD024020, 2016.

Hu, W., Day, D. A., Campuzano-Jost, P., Nault, B. A., Park, T., Lee, T., Croteau, P., Canagaratna, M. R., Jayne, J. T., Worsnop, D. R., and Jimenez, J. L.: Evaluation of the new capture vaporizer for aerosol mass spectrometers: Characterization of organic aerosol mass spectra, Aerosol Science and Technology, 52, 725–739, doi:10.1080/02786826.2018.1454584, 2018.

Hu, W. W., Hu, M., Yuan, B., Jimenez, J. L., Tang, Q., Peng, J. F., Hu, W., Shao, M., Wang, M., Zeng, L. M., Wu, Y. S., Gong, Z. H., Huang, X. F., and He, L. Y.: Insights on organic aerosol aging and the influence of coal combustion at a regional receptor site of central eastern China, Atmospheric Chemistry and Physics, 13, 10 095–10 112, doi:10.5194/acp-13-10095-2013, 2013.

Hu, W. W., Campuzano-Jost, P., Palm, B. B., Day, D. A., Ortega, A. M., Hayes, P. L., Krechmer, J. E., Chen, Q., Kuwata, M., Liu, Y. J., de Sá, S. S., McKinney, K., Martin, S. T., Hu, M., Budisulistiorini, S. H., Riva, M., Surratt, J. D., St. Clair, J. M., Isaacman-Van Wertz, G., Yee, L. D., Goldstein, A. H., Carbone, S., Brito, J., Artaxo, P., de Gouw, J. A., Koss, A., Wisthaler, A., Mikoviny, T., Karl, T., Kaser, L., Jud, W., Hansel, A., Docherty, K. S., Alexander, M. L., Robinson, N. H., Coe, H., Allan, J. D., Canagaratna, M. R., Paulot, F., and Jimenez, J. L.: Characterization of a real-time tracer for isoprene epoxydiols-derived secondary organic aerosol (IEPOX-SOA) from aerosol mass spectrometer measurements, Atmospheric Chemistry and Physics, 15, 11 807–11 833, doi:10.5194/acp-15-11807-2015, 2015.

Huang, C., Hu, Q., Wang, H., Qiao, L., Jing, S., Wang, H., Zhou, M., Zhu, S., Ma, Y., Lou, S., Li, L., Tao, S., Li, Y., and Lou, D.: Emission factors of particulate and gaseous compounds from a large cargo vessel operated under real-world conditions, Environmental Pollution, 242, 667–674, doi:10.1016/j.envpol.2018.07.036, 2018.

Jayne, J. T., Leard, D. C., Zhang, X., Davidovits, P., Smith, K. A., Kolb, C. E., and Worsnop, D. R.: Development of an Aerosol Mass Spectrometer for Size and Composition Analysis of Submicron Particles, Aerosol Science and Technology, 33, 49–70, doi:10.1080/027868200410840, 2000.

Le Berre, L., Temime-Roussel, B., Lanzafame, G. M., D'Anna, B., Marchand, N., Sauvage, S., Dufresne, M.,

Tinel, L., Leonardis, T., Ferreira de Brito, J., Armengaud, A., Gille, G., Lanzi, L., Bourjot, R., and Wortham, H.: Measurement report: In-depth characterization of ship emissions during operations in a Mediterranean port, EGUsphere, 2024, 1–44, doi:10.5194/egusphere-2024-2903, 2024.

Liu, P., Deng, R., Smith, K., Williams, L., Jayne, J., Canagaratna, M., Moore, K., Onasch, T., Worsnop, D., and Deshler, T.: Transmission Efficiency of an Aerodynamic Focusing Lens System: Comparison of Model Calculations and Laboratory Measurements for the Aerodyne Aerosol Mass Spectrometer, Aerosol Science and Technology - AEROSOL SCI TECH, 41, 721–733, doi:10.1080/02786820701422278, 2007.

Middlebrook, A. M., Bahreini, R., Jimenez, J. L., and and, M. R. C.: Evaluation of Composition-Dependent Collection Efficiencies for the Aerodyne Aerosol Mass Spectrometer using Field Data, Aerosol Science and Technology, 46, 258–271, doi:10.1080/02786826.2011.620041, 2012.

Mohr, C., DeCarlo, P. F., Heringa, M. F., Chirico, R., Slowik, J. G., Richter, R., Reche, C., Alastuey, A., Querol, X., Seco, R., Peñuelas, J., Jiménez, J. L., Crippa, M., Zimmermann, R., Baltensperger, U., and Prévôt, A. S. H.: Identification and quantification of organic aerosol from cooking and other sources in Barcelona using aerosol mass spectrometer data, Atmospheric Chemistry and Physics, 12, 1649–1665, doi:10.5194/acp-12-1649-2012, 2012.

Ng, N. L., Canagaratna, M. R., Zhang, Q., Jimenez, J. L., Tian, J., Ulbrich, I. M., Kroll, J. H., Docherty, K. S., Chhabra, P. S., Bahreini, R., Murphy, S. M., Seinfeld, J. H., Hildebrandt, L., Donahue, N. M., DeCarlo, P. F., Lanz, V. A., Prévôt, A. S. H., Dinar, E., Rudich, Y., and Worsnop, D. R.: Organic aerosol components observed in Northern Hemispheric datasets from Aerosol Mass Spectrometry, Atmospheric Chemistry and Physics, 10, 4625–4641, doi:10.5194/acp-10-4625-2010, 2010.

Quinn, P. K., Bates, T. S., Coffman, D., Onasch, T. B., Worsnop, D., Baynard, T., de Gouw, J. A., Goldan, P. D., Kuster, W. C., Williams, E., Roberts, J. M., Lerner, B., Stohl, A., Pettersson, A., and Lovejoy, E. R.: Impacts of sources and aging on submicrometer aerosol properties in the marine boundary layer across the Gulf of Maine, Journal of Geophysical Research: Atmospheres, 111, doi:10.1029/2006JD007582, 2006.

Saarikoski, S., Carbone, S., Decesari, S., Giulianelli, L., Angelini, F., Canagaratna, M., Ng, N. L., Trimborn, A., Facchini, M. C., Fuzzi, S., Hillamo, R., and Worsnop, D.: Chemical characterization of springtime submicrometer aerosol in Po Valley, Italy, Atmospheric Chemistry and Physics, 12, 8401–8421, doi:10.5194/acp-12-8401-2012, 2012.

Setyan, A., Zhang, Q., Merkel, M., Knighton, W. B., Sun, Y., Song, C., Shilling, J. E., Onasch, T. B., Herndon, S. C., Worsnop, D. R., Fast, J. D., Zaveri, R. A., Berg, L. K., Wiedensohler, A., Flowers, B. A., Dubey, M. K., and Subramanian, R.: Characterization of submicron particles influenced by mixed biogenic and anthropogenic emissions using high-resolution aerosol mass spectrometry: results from CARES, Atmospheric Chemistry and Physics, 12, 8131–8156, doi:10.5194/acp-12-8131-2012, 2012.

Shah, R. U., Robinson, E. S., Gu, P., Robinson, A. L., Apte, J. S., and Presto, A. A.: High-spatial-resolution mapping and source apportionment of aerosol composition in Oakland, California, using mobile aerosol mass spectrometry, Atmospheric Chemistry and Physics, 18, 16 325–16 344, doi:10.5194/acp-18-16325-2018, 2018.

Sinha, P., Hobbs, P. V., Yokelson, R. J., Christian, T. J., Kirchstetter, T. W., and Bruintjes, R.: Emissions of trace gases and particles from two ships in the southern Atlantic Ocean, Atmospheric Environment, 37, 2139–2148, doi:10.1016/S1352-2310(03)00080-3, 2003.

Struckmeier, C., Drewnick, F., Fachinger, F., Gobbi, G. P., and Borrmann, S.: Atmospheric aerosols in Rome, Italy: sources, dynamics and spatial variations during two seasons, Atmospheric Chemistry and Physics, 16, 15 277–15 299, doi:10.5194/acp-16-15277-2016, 2016.

Timonen, H., Teinilä, K., Barreira, L., Simonen, P., Dal Maso, M., Keskinen, J., Kalliokoski, J., Moldonova, J., Salberg, H., Merelli, L., D'Anna, B., Temime-Roussel, B., Lanzafame, G. M., and Mellqvist, J.: Ship on-board emissions characterisation, Technical report, The SCIPPER Project, https://www.scipper-project.eu/library/, 2022.

Volent, E., Gunti, Q., D'Anna, B., Brito, J. F. D., Jamar, M., Temime-Roussel, B., Moldanova, J., Timonen, H., Hellen, H., Lanzafame, G., Maso, M. D., Rozé, S., Riffault, V., Tinel, L., and Sauvage, S.: Determining Volatile Organic Compounds and PM_1 Emission Factors from land-based, high time-resolution observations in an Emission Control Area of northern France, in preparation, 2025.

Voliotis, A., Wang, Y., Shao, Y., Du, M., Bannan, T. J., Percival, C. J., Pandis, S. N., Alfarra, M. R., and McFiggans, G.: Exploring the composition and volatility of secondary organic aerosols in mixed anthropogenic and biogenic precursor systems, Atmospheric Chemistry and Physics, 21, 14 251–14 273, doi:10.5194/acp-21-14251-2021, 2021.

Wang, L., Du, W., Shen, H., Chen, Y., Zhu, X., Yun, X., Shen, G., Chen, Y., Liu, J., Wang, X., and Tao, S.: Unexpected Methane Emissions From Old Small Fishing Vessels in China, Frontiers in Environmental Science, 10, doi:10.3389/fenvs.2022.907868, 2022.

Winnes, H., Moldanová, J., Anderson, M., and Fridell, E.: On-board measurements of particle emissions from marine engines using fuels with different sulphur content, Proceedings of the Institution of Mechanical Engineers, Part M: Journal of Engineering for the Maritime Environment, 230, 45–54, doi:10.1177/1475090214530877, 2016.

Zhang, Y., Heikkinen, L., Äijälä, M., Peräkylä, O., Graeffe, F., Mickwitz, V., Zhao, J., Daellenbach, K., Sueper, D., Worsnop, D., Riva, M., and Ehn, M.: Enhanced Aerosol Source Identification by Utilizing High Molecular Weight Signals in Aerosol Mass Spectra, ACS ES&T Air, doi:10.1021/acsestair.3c00102, 2024.